Table 1 Relationship between luminal subtypes and clinicopathological characteristics

	Luminal A ($n = 106$)[a]	Luminal B ($n = 74$)[a]	P value
Menopausal status			
Pre-	36 (56)[b]	28 (44)	0.59
Post-	70 (60)	46 (40)	
Tumor size			
≤2 cm	71 (65)	39 (35)	0.05
>2 cm	35 (50)	35 (50)	
Histological type			
IDC	90 (57)	69 (43)	0.06
ILC	7 (100)	0 (0)	
Others	9 (64)	5 (36)	
Lymph node metastasis			
No	76 (62)	46 (38)	0.17
Yes	30 (52)	28 (48)	
Nuclear grade			
1	84 (73)	31 (27)	<0.0001
2	18 (49)	19 (51)	
3	4 (14)	24 (86)	
ER expression levels[c]	90.4 (70.5–100)	87.7 (50–100)	0.22
PR expression levels[c]	55.2 (9.4–84.7)	24.8 (5.0–60.0)	0.04

IDC invasive ductal carcinoma, *ILC* invasive lobular carcinoma

[a] Luminal A: Ki67 <14%, luminal B: Ki67 ≥14%, [b] values in parentheses indicate percentage, [c] % of positive nuclei, median (25th and 75th percentiles)

milieu, however, local production of estrogens may not be sufficient in all cancers and because of relatively lower estrogens cannot induce high levels of PR. Similar with this observation, Yamashita et al. [7] have reported that the frequency of ER-positive and PR-negative cancers in Japanese women over 50 years (14%) was higher than in women aged 50 years or younger (5%).

On the basis of these observations, we speculate the difference between pre- and postmenopausal ER-H/PR-L cancers depends on a mechanism such as the one described above. This hypothesis seems to be partly supported by our observation that ER and PR expression levels strongly correlate in premenopausal luminal A cancers, but only weakly so in postmenopausal luminal A cancers (Fig. 2). As also shown in this figure, a large number of cancers are plotted in the ER-H/PR-L area among postmenopausals. Haynes et al. [8] demonstrated that mRNA expression levels of PR were significantly associated with intratumoral estradiol concentrations in postmenopausal patients. The findings of this study point to the importance of local synthesis of estradiol for PR expression in postmenopausal breast cancers. In order to reach a definitive answer to this issue, direct comparison between intratumoral estradiol levels and PR expression levels is needed. However, we were unable to obtain enough fresh tissues for this assay.

The frequency of ER-L/PR-L in premenopausal luminal A cancers (19%) was higher than that in postmenopausal luminal A cancers (6%). Estrogen independence in ER-positive cancers and the accompanying induction of growth factor signaling have led to the recognition of ER downregulation in both in vitro and in vivo studies [9, 10]. Moreover, under conditions of excessive estrogen, ER downregulation has also been demonstrated in a previous in vitro study [11]. The reason for the high frequency of ER-L/PR-L in premenopausals may be ER downregulation caused by an excessive estrogen supply because crosstalk with growth factor signaling is less likely in luminal A cancers. Although it is not known whether ER is downregulated by high levels of estrogen in all human breast cancer, such downregulation may occur in premenopausal breast cancers. Thus, the difference in the distribution of ER and PR expression levels between pre- and postmenopausals among luminal A cancers may depend on the estrogen environment. As shown in Fig. 1 and Table 2, luminal B cancers are most frequently involved in premenopausal ER-H/PR-L and postmenopausal ER-L/PR-L cancers. Interestingly, the distribution of ER and PR expression levels was similar for pre- and postmenopausal luminal B cancers, and this finding may indicate that growth factor signaling has a stronger influence than estrogen signaling on the expression of ER and PR.

In conclusion, we were able to identify biological differences between luminal A and luminal B cancers. The estrogen environment appears to have a strong effect on ER and PR expression levels of luminal A, but seems to be less important for luminal B cancers. Determination of Ki67 expression levels may thus be useful for evaluation of estrogen dependency, especially of postmenopausal ER-H/PR-L cancers. It is hoped these findings will prove to be useful for a further understanding of the biological

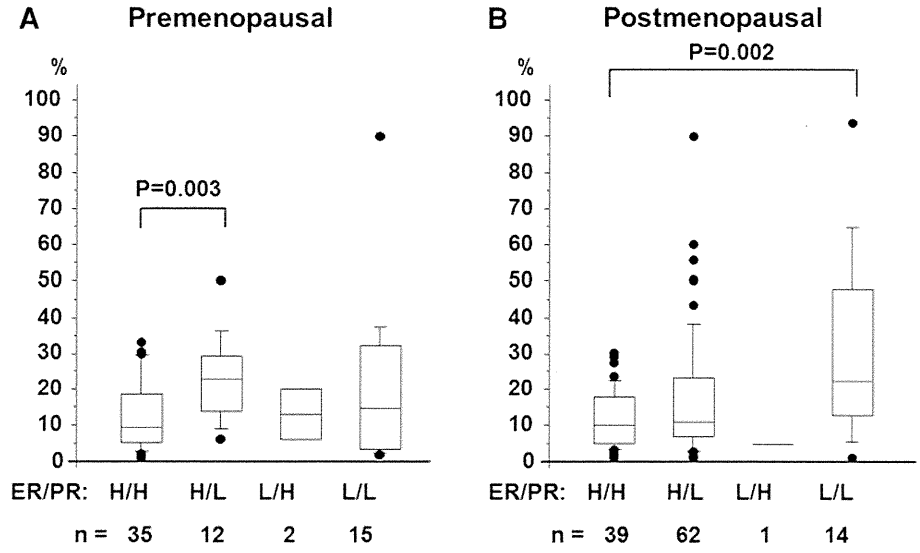

Fig. 1 Ki67 labeling index for ER and PR expression levels in premenopausals (**a**) and postmenopausals (**b**). *H* more than 50% nuclear staining, *L* 50% or less nuclear staining

Table 2 ER, PR expression levels and menopausal status in luminal A and luminal B subtypes

	Premenopausals	Postmenopausals	*P* value
Luminal A[a]			
ER-H and PR-H[b]	25 (69)[c]	27 (39)	0.0001
ER-H and PR-L[b]	3 (8)	38 (54)	
ER-L and PR-H	1 (3)	1 (1)	
ER-L and PR-L	7 (19)	4 (6)	
Luminal B[a]			
ER-H and PR-H	10 (36)	12 (26)	0.25
ER-H and PR-L	9 (32)	24 (52)	
ER-L and PR-H	1 (4)	0 (0)	
ER-L and PR-L	8 (29)	10 (22)	

[a] Luminal A: Ki67 <14%, luminal B: Ki67 ≥14%. [b]H: more than 50% nuclear staining; L: 50% or less nuclear staining, [c] values in parentheses indicate percentage

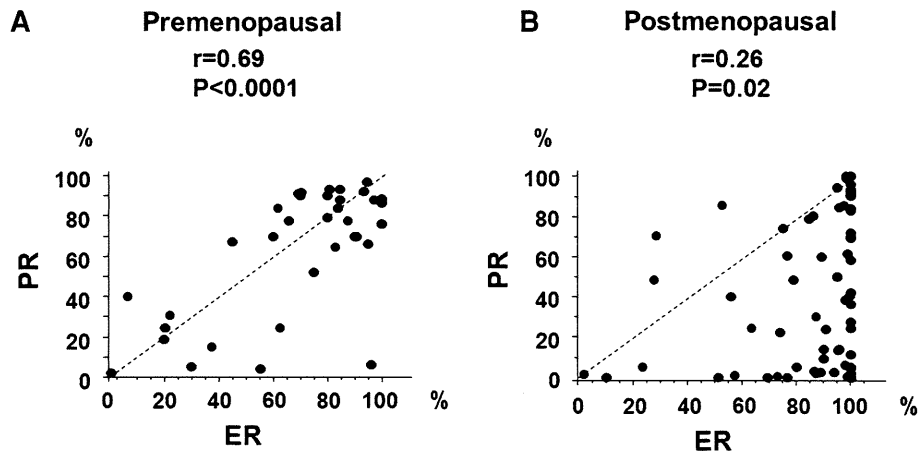

Fig. 2 Correlation between ER and PR expression levels in premenopausal (**a**) and postmenopausal (**b**) luminal A cancers

characteristics of luminal A and luminal B cancers. In order to resolve these issues definitively, studies including larger numbers of patients as well as an investigation of the correlation of the biological characteristics with prognosis need to be done in future.

Conflict of interest Officers or advisers of companies or for-profit organizations: Dr. Toyomasa Katagiri (Memeber of the Board of Oncotherapy Science Co., Ltd). Honoraria paid by companies or for-profit organization as compensation for time or labor of researcher engaged for conference attendance: Dr. Yasuo Miyoshi (Astrazeneca K.K., Taiho Pharmaceutical Co., Ltd, Novartis K.K.).

References

1. Perou CM, Sørlie T, Eisen MB, van de Rijn M, Jeffrey SS, Rees CA, et al. Molecular portraits of human breast tumours. Nature. 2000;406:747–52.
2. Cheang MC, Chia SK, Voduc D, Gao D, Leung S, Snider J, et al. Ki67 index, HER2 status, and prognosis of patients with luminal B breast cancer. J Natl Cancer Inst. 2009;101:736–50.
3. Goldhirsch A, Wood WC, Coates AS, Gelber RD, Thürlimann B, Senn HJ. Strategies for subtypes-dealing with the diversity of breast cancer: highlights of the St Gallen International Expert Consensus on the Primary Therapy of Early Breast Cancer 2011. Ann Oncol. 2011;22:1736–47.
4. Early Breast Cancer Trialists' Collaborative Group (EBCTCG). Effects of chemotherapy and hormonal therapy for early breast cancer on recurrence and 15-year survival: an overview of the randomised trials. Lancet. 2005;365:1687–717.
5. Cui X, Zhang P, Deng W, Oesterreich S, Lu Y, Mills GB, et al. Insulin-like growth factor-I inhibits progesterone receptor expression in breast cancer cells via the phosphatidylinositol 3-kinase/Akt/mammalian target of rapamycin pathway: progesterone receptor as a potential indicator of growth factor activity in breast cancer. Mol Endocrinol. 2003;17:575–88. Erratum in: Mol Endocrinol. 2003;17:1892
6. Sakamoto G, Inaji H, Akiyama F, Haga S, Hiraoka M, Inai K, et al. Japanese Breast Cancer Society. General rules for clinical and pathological recording of breast cancer 2005. Breast Cancer. 2005;12(Suppl):S1–27.
7. Yamashita H, Iwase H, Toyama T, Takahashi S, Sugiura H, Yoshimoto N, et al. Estrogen receptor-positive breast cancer in Japanese women: trends in incidence, characteristics, and prognosis. Ann Oncol. 2011;22:1318–25.
8. Haynes BP, Straume AH, Geisler J, A'Hern R, Helle H, Smith IE, et al. Intratumoral estrogen disposition in breast cancer. Clinical Cancer Res. 2010;16:1790–801.
9. Brodie A, Sabnis G, Jelovac D. Aromatase and breast cancer. J Steroid Biochem Mol Biol. 2006;102:97–102.
10. Sabnis GJ, Macedo LF, Goloubeva O, Schayowitz A, Brodie AM. Stopping treatment can reverse acquired resistance to letrozole. Cancer Res. 2008;68:4518–24.
11. Harrell JC, Dye WW, Harvell DM, Pinto M, Jedlicka P, Sartorius CA, et al. Estrogen insensitivity in a model of estrogen receptor-positive breast cancer lymph node metastasis. Cancer Res. 2007;67:10582–91.

Current Biology 22, 1659–1666, September 25, 2012 ©2012 Elsevier Ltd All rights reserved http://dx.doi.org/10.1016/j.cub.2012.07.034

Article

A DNA-Damage Selective Role for BRCA1 E3 Ligase in Claspin Ubiquitylation, CHK1 Activation, and DNA Repair

Ko Sato,[1] Elayanambi Sundaramoorthy,[1] Eeson Rajendra,[1] Hiroyoshi Hattori,[1] Anand D. Jeyasekharan,[1] Nabieh Ayoub,[1] Ralph Schiess,[2] Ruedi Aebersold,[2] Hiroyuki Nishikawa,[3] Anna S. Sedukhina,[3] Haruka Wada,[4] Tomohiko Ohta,[3] and Ashok R. Venkitaraman[1,*]

[1]University of Cambridge, Medical Research Council Cancer Cell Unit, Hutchison/MRC Research Centre, Hills Road, Cambridge CB2 OXZ, UK

[2]Institute of Molecular Systems Biology, Eidgenössische Technische Hochschule (ETH) Zurich, 8093 Zurich, Switzerland

[3]Institute of Advanced Medical Science and Department of Translational Oncology, St. Marianna University Graduate School of Medicine, Kawasaki 216-8511, Japan

[4]Division of Immunobiology, Institute of Genetic Medicine Hokkaido University, Sapporo 060-0815, Japan

Summary

Background: The breast and ovarian cancer suppressor BRCA1 is essential for cellular responses to DNA damage [1]. It heterodimerizes with BARD1 to acquire an E3 ubiquitin (Ub) ligase activity that is often compromised by cancer-associated mutations [2]. Neither the significance of this activity to damage responses, nor a relevant in vivo substrate, is clear.

Results: We have separated DNA-damage responses requiring the BRCA1 E3 ligase from those independent of it, using a gene-targeted point mutation in vertebrate DT40 cells that abrogates BRCA1's catalytic activity without perturbing BARD1 binding. We show that BRCA1 ubiquitylates claspin, an essential coactivator of the CHK1 checkpoint kinase, after topoisomerase inhibition, but not DNA crosslinking by mitomycin C. BRCA1 E3 inactivation decreases chromatin-bound claspin levels and impairs homology-directed DNA repair by interrupting signal transduction from the damage-activated ATR kinase to its effector, CHK1.

Conclusions: Our findings identify claspin as an in vivo substrate for the BRCA1 E3 ligase and suggest that its modification selectively triggers CHK1 activation for the homology-directed repair of a subset of genotoxic lesions. This mechanism unexpectedly defines an essential but selective function for BRCA1 E3 ligase activity in cellular responses to DNA damage.

Introduction

There is abundant evidence that the breast and ovarian tumor suppressor, BRCA1, has essential functions in diverse cellular processes implicated in the DNA damage response [1]. How BRCA1 mediates these functions remains unclear. Much attention has focused on the E3 ubiquitin ligase activity acquired when BRCA1 heterodimerizes through its amino-terminal RING domain with an evolutionarily conserved RING partner, BARD1 [3]. Deleterious missense mutations affecting the BRCA1 RING domain can be found in familial breast cancers that do not vitiate BARD1 binding but can nevertheless abolish E3 ligase activity [2, 4], suggestive of its functional importance. However, a BRCA1 point mutation abolishing E3 activity does not impair ionizing radiation sensitivity or the repair of endonuclease-induced DNA breaks by homologous recombination [5]. Furthermore, mice harboring the mutation do not develop breast cancers [6]. On the other hand, inactivation of BRCA1 E3 ligase activity can derepress heterochromatic satellite DNA transcription, an event that has been linked to abnormalities in DNA repair and mitosis [7]. Thus, if and how BRCA1's E3 ligase activity is necessary for the cellular response to DNA damage remains uncertain.

BRCA1 has been implicated in several processes essential for the cellular response to DNA lesions repaired by homologous recombination [1]. One key step involves activation of the checkpoint kinase CHK1, an essential component of the damage response machinery in vertebrates. Phosphorylation of CHK1 occurs on chromatin. The phosphorylated CHK1 is released from chromatin and the dissociation is required for checkpoint activation [8]. BRCA1 has been implicated in CHK1 activation via ATR and claspin. ATR-phosphorylated claspin forms a trimolecular complex containing BRCA1 and CHK1 [9]. Complex formation is essential for CHK1 phosphorylation and activation [9]; in turn, activated CHK1 mediates checkpoint enforcement as well as DNA repair by homologous recombination [10, 11], through modulation of the interaction between BRCA2 and the recombinase RAD51 [12, 13]. However, the mechanism through which BRCA1 controls the claspin-CHK1 axis, and in particular, whether its E3 ligase activity is required, is not known.

Here, we have used "hit-and-run" gene targeting to create a DT40 cell line carrying a single mutation in BRCA1, replacing Val26 in the RING domain with Ala (V26A). The V26A mutation abrogates E3 ligase activity without affecting the interaction between BRCA1 and BARD1. Unexpectedly, E3 inactivation reveals a mechanism distinguishing DNA damage responses that require BRCA1's catalytic activity, from those independent of it. Whereas the BRCA1 E3 ligase is essential for chromatin association of claspin and CHK1 activation when a topoisomerase poison, camptothecin (CPT), blocks DNA replication, it is dispensable for these events after replication blockage by a DNA crosslinker, mitomycin C (MMC). In turn, downstream responses regulated by CHK1, including RAD51 foci formation, sister chromatid exchange, and cellular sensitivity, are selectively impaired after exposure to CPT, but not MMC. Thus, our work suggests that the BRCA1 E3 ligase selectively triggers claspin-CHK1 activation, providing the first example of an E3-dependent mechanism underlying an essential function for BRCA1 in the cellular response to DNA damage.

Results and Discussion

BRCA1 has been implicated in the cellular response to DNA double-strand breaks leading to their resolution by homology-directed repair (HDR) [1]. We used avian DT40 cells, a well-established model widely used to study the role of BRCA1 in this response [14–16], to determine the functional

*Correspondence: arv22@cam.ac.uk

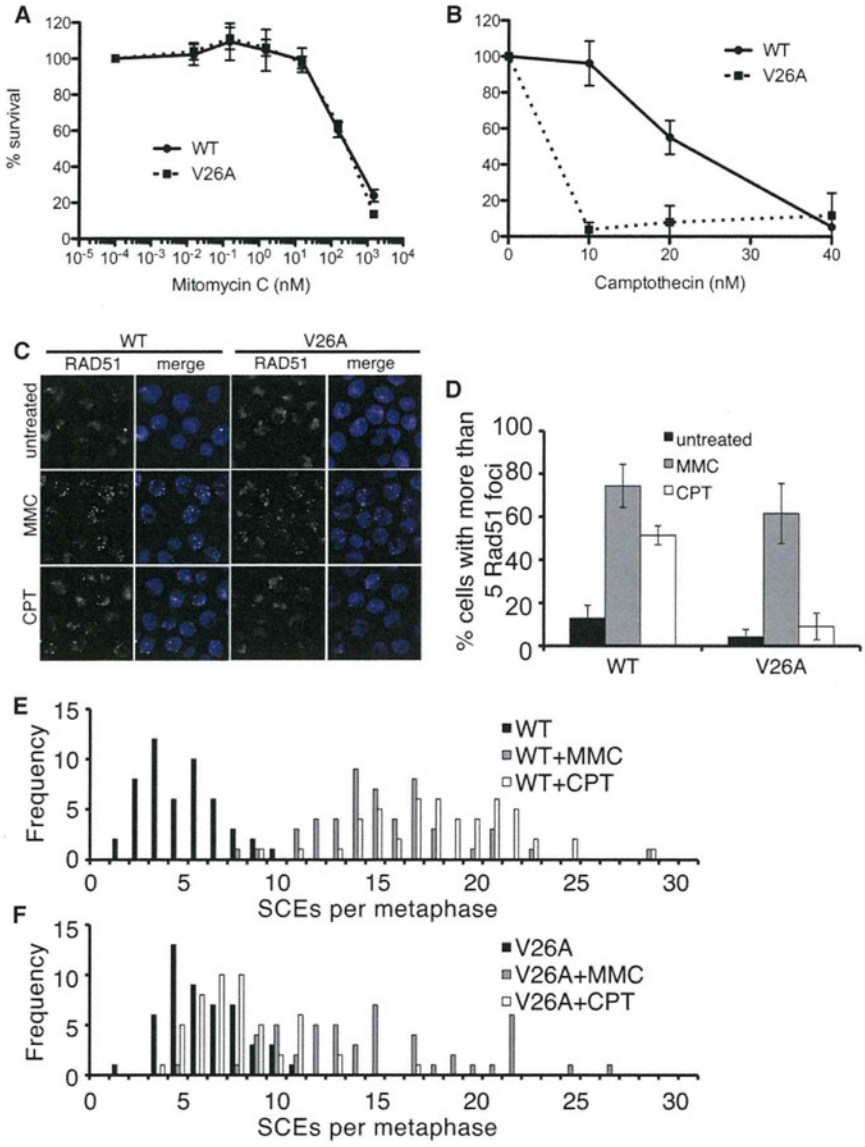

Figure 1. The V26A Point Mutation Defines a Subset of Genotoxic Responses Requiring BRCA1 E3 Ligase Activity

(A and B) Cell viability, as determined by the CellTiter Blue colorimetric assay, is expressed as a percentage of the untreated control sample for both cell lines. The percentage of viable cells is plotted for each of the indicated doses of mitomycin C (MMC) (A) and camptothecin (CPT) (B). Error bars (some too small to be visible) show the SD from the mean of four independent wells from three independent experiments.

(C) Representative micrographs of WT or V26A DT40 cells, undamaged (top row) or treated for 6 hr with the indicated drugs (rows 2–4) and stained with anti-RAD51 (grayscale). DNA staining was with DAPI (blue).

(D) Histogram showing the percentage of cells with >5 RAD51 foci. RAD51 foci were counted in WT and V26A cells (n = 100) before and after exposure to the indicated drugs (MMC: 150 nM for 8 hr, CPT: 100 nM for 8 hr). Error bars show the SD from the mean of three independent experiments.

(E and F) Histograms showing the frequency distribution for spontaneous, MMC (150 nM for 8 hr) or CPT (100 nM for 8 hr)-induced sister chromatid exchanges (SCE's) in WT (E) or V26A DT40 cells (F). Spontaneous SCE formation is intact, but only MMC (gray color bars) induces SCEs in V26A mutant cells. See also Figure S1 and Table S1.

significance of BRCA1 E3 ligase activity. In mammalian BRCA1 homologs, Ile26 in the RING domain is implicated in binding to E2 ubiquitin conjugating enzymes [2]. Its substitution by Ala abolishes BRCA1's E3 ligase activity without affecting heterodimerization to BARD1 [2]. Val26 in the avian RING domain conservatively replaces Ile26 in its mammalian counterparts, reflecting their strong evolutionary conservation (see Figure S1A available online). We cloned the RING domains of avian BRCA1 and BARD1 from a DT40 complementary DNA (cDNA) library and introduced the Val26Ala (V26A) point mutation by site-directed mutagenesis. When cotransfected into 293T cells with the avian BARD1 RING domain, the V26A mutant form of the *Gg*BRCA1 RING domain still binds to the BARD1 RING domain (Figure S1B) but fails to catalyze the transfer of ubiquitin in vitro (Figure S1C). Thus, replacement of Val26 with Ala in avian BRCA1 abolishes the E3 ligase activity of the RING domain but not its interaction with BARD1. This confirms that avian Val26 is functionally cognate with Ile26 in mammalian BRCA1.

Figure S1D shows the gene-targeting strategy used to create a DT40 cell line carrying a Val26-Ala substitution in the endogenous *BRCA1* gene. The targeting vector carries a blasticidin or neomycin resistance cassette flanked by *loxP* sites for the CRE recombinase, enabling recycling of the resistance marker by CRE transfection between sequential rounds of targeted integration. Homozygous Val26-Ala replacement was confirmed by amplification of the targeted *BRCA1* genomic locus using the indicated primers (Figure S1D), by a diagnostic restriction digest with BsrDI (Figure S1E) and by nucleotide sequencing (data not shown). Western blotting of extracts from BRCA1 wild-type (WT) or BRCA1$^{V26A/V26A}$ (V26A) cells confirmed that the WT and mutant BRCA1 proteins were expressed at similar levels (Figures S1F and S1G). Thus, in accord with previous reports [14, 15], BRCA1 E3 ligase is dispensable for the viability and growth of DT40 cells.

BRCA1 has been implicated in the cellular response to agents that inflict DNA lesions repaired by HDR. These include the topoisomerase I poison, camptothecin (CPT), which triggers DNA breakage at replication forks [17], or the DNA crosslinking agent, mitomycin C (MMC), which creates intrastrand lesions as well as interstrand crosslinks that prevent the movement of replication forks [18]. We exposed WT or V26A cells to increasing doses of CPT or MMC for 40 hr before measuring cell viability (Figures 1A and 1B). V26A cells exhibit enhanced sensitivity to CPT, but not MMC. This raises the unexpected possibility that BRCA1 E3 ligase activity is selectively required for certain cellular responses leading to the repair of certain types of DNA lesions by HDR, but not others.

Two key cellular events report on the integrity of HDR in DT40 cells. First, inactivating mutations in known HDR

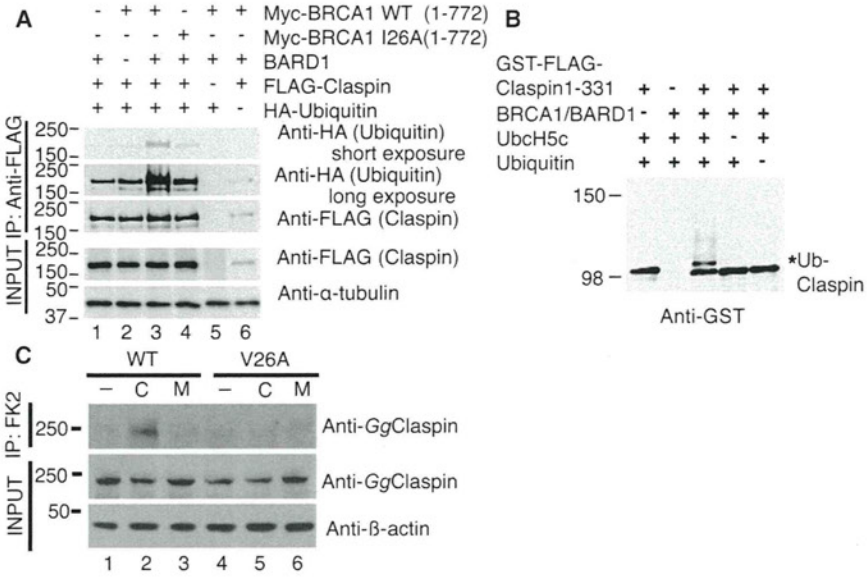

Figure 2. BRCA1 Ubiquitylates Claspin In Vitro and In Vivo in Cells Exposed to CPT but Not MMC

(A) 293T cells were transfected with constructs encoding FLAG-claspin, a myc-tagged BRCA1 fragment spanning residues 1–772 (myc-BRCA1 1–772 WT or I26A mutant), BARD1, or HA-ubiquitin as indicated. Cell lysates were prepared 24 hr afterward, immunoprecipitated with anti-FLAG antibody, and blotted with anti-HA and anti-FLAG antibodies, as indicated. The HA-tagged, ubiquitylated form of FLAG-claspin is present only when both myc-BRCA1 WT 1–772 and BARD1 are coexpressed. Whole-cell lysates were immunoblotted with anti-FLAG to show the expression level of FLAG-claspin and with anti-α-tubulin as a loading control.

(B) In vitro ubiquitin ligation assay was performed with a GST-FLAG tagged claspin fragment spanning residues 1–331 (GST-FLAG claspin 1–331), E1, UbcH5c, ubiquitin, and BRCA1/BARD1 RING heterodimeric complex as indicated, in the presence of ATP. Reaction products were immunoblotted with anti-GST antibody.

(C) WT or V26A DT40 cells were treated with CPT (100 nM) for 3 hr or MMC (150 nM) for 6 hr. Cell lysates were immunoprecipitated with FK2 (anti-conjugated ubiquitin antibody) and western blotted with anti-*Gg*claspin. "C" and "M" indicate treatment with CPT and MMC respectively. Ubiquitin-conjugated claspin was detected only in CPT-treated WT cells (top panel). Blotting with anti-β-actin serves as a loading control. See also Figure S2.

proteins, including BRCA1 deletions [14], suppress the accumulation of the recombination enzyme RAD51 in nuclear foci at sites of DNA repair. Second, such mutations also inhibit the spontaneous or genotoxin-induced exchange of genetic material between sister chromatids (sister chromatid exchange, SCE), a direct measure of HDR [19]. Consistent with their enhanced sensitivity to CPT, V26A cells exhibit a diminution in their ability to form RAD51 foci in response to these agents, when compared to WT cells (Figures 1C and 1D). Interestingly, such a defect is not apparent when these cell lines are exposed to MMC, consistent with their lack of sensitivity to this genotoxin. Similarly, the V26A mutation in BRCA1 also suppresses SCE formation induced by CPT, but not MMC (Figures 1E and 1F; Table S1) even though spontaneous SCE formation in V26A cells is slightly greater than in WT controls. Because SCE formation is a direct measure of crossover events mediated by HDR [19], our findings indicate that BRCA1 E3 activity is dispensable for the execution of DNA repair by this pathway in response to spontaneously arising, or MMC-induced, DNA damage. Instead, they reveal a more selective requirement for BRCA1's catalytic activity in the repair of CPT-induced lesions by HDR.

To identify substrates for BRCA1 E3 ligase relevant to this dichotomous role, we examined claspin, a critical coactivator of the damage-activated checkpoint kinase CHK1 necessary for HDR [9, 20]. BRCA1 forms a trimolecular complex with CHK1 and claspin through its direct binding to claspin, although how it promotes their activation remains unknown [9]. We therefore tested whether claspin itself might be an unrecognized target for modification by the E3 ligase activity of BRCA1. A myc-tagged fragment spanning residues 1 to 772 of BRCA1, which forms an active E3 ligase enzyme when cotransfected with BARD1 [3], can conjugate hemagglutinin (HA)-tagged ubiquitin (Ub) to FLAG-claspin (Figure 2A). This activity is abrogated by omission of either BARD1 or BRCA1, or expression of the BRCA1 I26A mutant, confirming that claspin modification requires the heterodimeric E3 enzyme. To identify the regions of claspin that can undergo modification, we first tested four fragments each of about 350 amino acids dividing claspin at well-established domain boundaries [21]. The N-terminal fragment spanning residues 1–331 was highly ubiquitylated compared to other fragments (data not shown). The copurified recombinant BRCA1/BARD1 heterodimeric complex is able to ubiquitylate this N-terminal claspin fragment in an in vitro Ub ligation assay (Figure 2B), indicating that it is a candidate substrate for the BRCA1 E3 ligase.

Many candidate substrates for the BRCA1 E3 ligase have been identified in vitro, but none has so far been confirmed in cellular studies [22]. We therefore asked whether claspin ubiquitylation could be detected in cells and whether this modification reflected the dichotomous requirement we have identified for BRCA1 E3 ligase activity in the response to CPT but not MMC. We exposed WT or V26A cells to these agents before cell lysates were immunoprecipitated with an antibody to conjugated ubiquitin (FK2), followed by western blotting with an anti-*Gg*claspin antibody. Strikingly, the Ub conjugation of endogenous claspin was induced in response to CPT (but not MMC) in WT (but not V26A) cells (Figure 2C). One predominant Ub-conjugated claspin species is observed, consistent with our overexpression experiments in 293T, in which FLAG-claspin was modified with HA-ubiquitin (Figure 2A). These observations suggest that the BRCA1 E3 ligase does indeed selectively ubiquitylate claspin in cells exposed to CPT but not MMC, and provide a first example of in vivo substrate ubiquitylation by this enzyme during a biological process.

We identified the sites of BRCA1/BARD1-mediated ubiquitin conjugation in the N-terminal claspin fragment spanning residues 1–331 by mass spectrometry (Figures 3A and 3B; Table S2). Analysis of tryptic digests of this claspin fragment after in vitro ubiquitylation by BRCA1/BARD1 revealed four potential conjugation sites (Table S2). Covalent linkage of a di-Gly motif introduced by substrate ubiquitylation at Lys60 and Lys96 was unambiguously identified in two independent fragment-ion spectra each, whereas Lys89 and Lys105 were identified in only one spectrum each (Figures 3A and 3B).

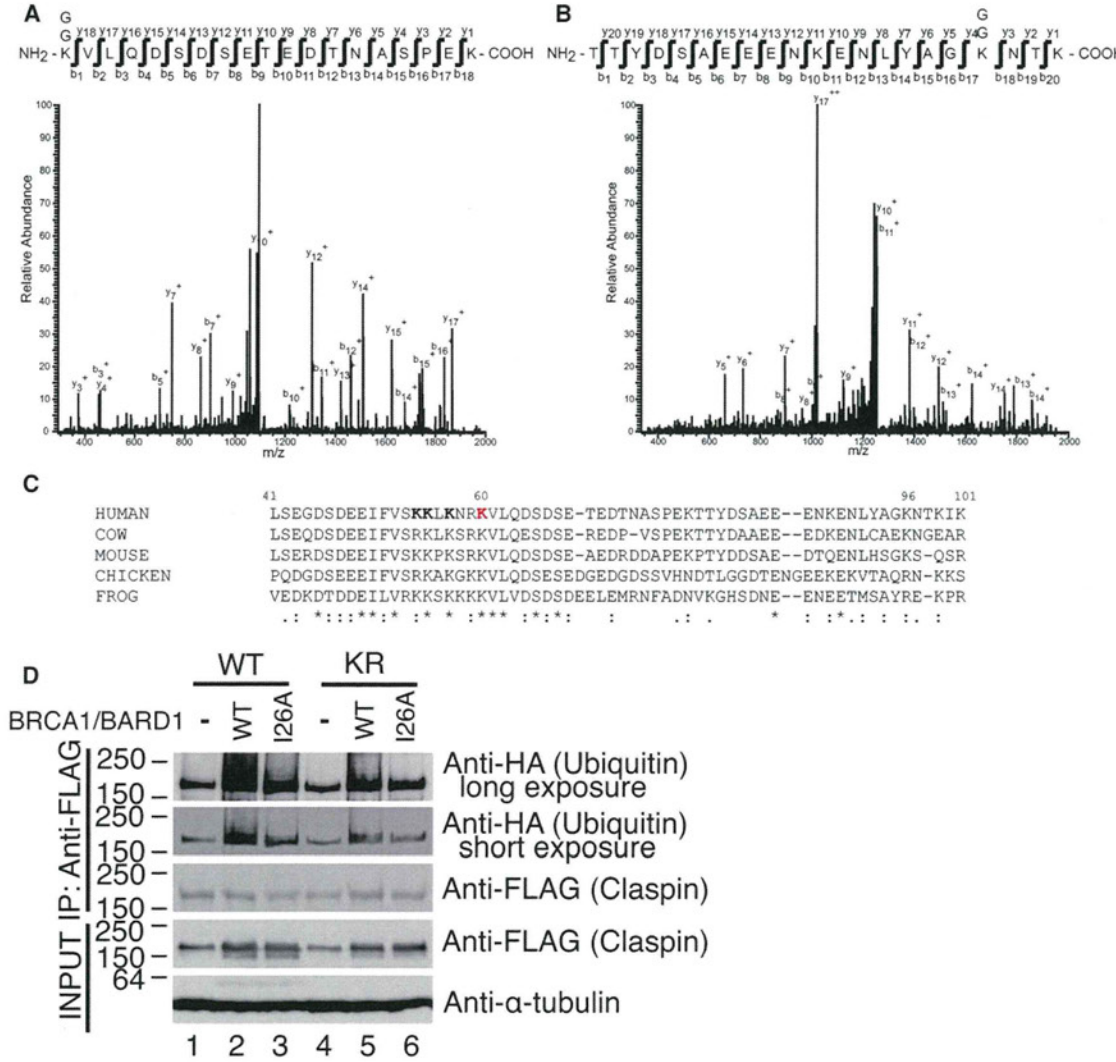

Figure 3. BRCA1-Mediated Claspin Ubiquitylation Targets N-Terminal Lys Residues

(A and B) The fragment ion spectra show the claspin tryptic peptides K*VLQDSDSETEDTNASPEK (A) and TTYDSAEEENKENLYAGK*NTK (B) and confirm the presence of a double glycine (GG) modification at Lys-60 as well as at Lys-96, assigning unambiguously the site of ubiquitylation (indicated by an asterisk modification).

(C) Multispecies protein sequence alignment of amino-terminal claspin residues 41–101. * indicates that the residues are identical. ":" indicates that residues have conserved substitutions. Lysine residues highlighted in bold were mutated to arginine.

(D) 293T cells were transfected with FLAG-claspin (WT or the NT-KR mutant), HA-ubiquitin, myc-BRCA1 1–772 (WT or I26A mutant), and BARD1 as indicated. Cell lysates were subjected to sequential immunoprecipitation and western blotting with anti-FLAG and anti-HA antibodies respectively. Five percent of the input per immunoprecipitation was blotted with the indicated antibodies. Ubiquitylation of the NT-KR claspin mutant is reduced compared to WT. See also Figure S3 and Table S2.

Moreover, a protein sequence alignment of residues 1–331 of claspin across multiple species that also have a known BRCA1 ortholog demonstrated that Lys60 was found in a region of high sequence conservation that also contained additional conserved basic residues. In contrast, the sequence surrounding Lys96 is less well conserved (Figure 3C). Taken collectively, these findings suggest that Lys60 represents an evolutionarily conserved modification site on claspin, and that the protein may also be modified by Ub conjugation at additional Lys residues in its N-terminal region.

In fact, three conserved lysines (Lys54, Lys55, and Lys57) occur in the six residues N-terminal to Lys60. Because site-specific ubiquitylation becomes promiscuous if the preferred Lys target is absent but a neighboring alternative acceptor lysine is present [23], we created a mutant form of claspin (NT-KR) in which all four Lys residues at positions 54, 55, 57, and 60 were changed to Arg. WT or NT-KR mutant forms of claspin were cotransfected into 293T cells with BRCA1/BARD1 in the presence of HA-ubiquitin. Ub conjugation to WT claspin was evident when BRCA1/BARD1 were coexpressed, and decreased by expression of the BRCA1 I26A mutant (Figure 3D). Moreover, the NT-KR claspin mutant shows reduced modification compared to the WT form. Together, these data suggest that BRCA1/BARD1 conjugates Ub to Lys60 and adjacent residues in the N-terminus of claspin.

Because CHK1 is phosphorylated on chromatin when forming a complex with BRCA1 and claspin, we tested whether

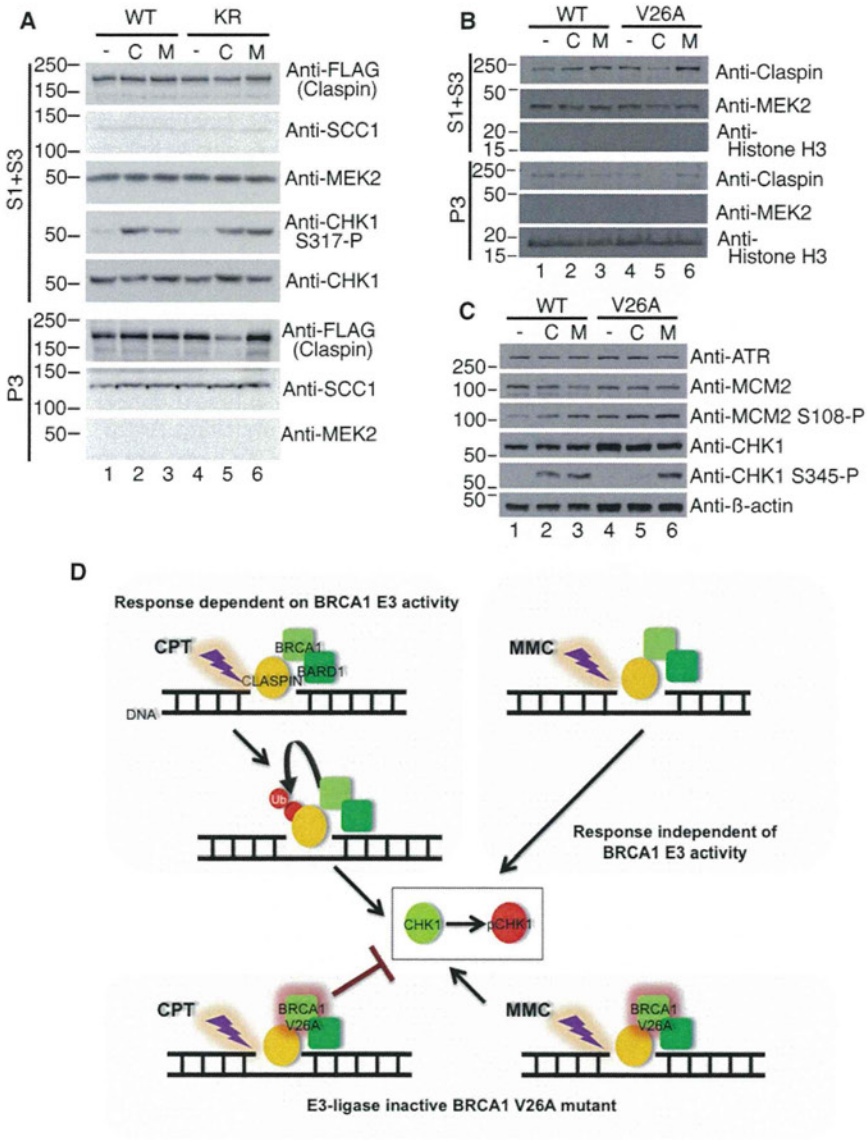

Figure 4. BRCA1 E3 Inactivation Decreases Chromatin-Bound Claspin and Suppresses CHK1 Activation Specifically in Response to CPT but Not MMC

(A) 293T cells were transfected with constructs encoding either WT or NT-KR mutant forms of claspin. Thirty-six hours after transfection, cells were fractionated into cytoplasmic and nuclear soluble (S1 + S3) or chromatin-bound (P3) fractions, and immunoblotted with the indicated antibodies. SCC1 and MEK2 serve as controls for loading and the effectiveness of fractionation. "C" and "M" indicate treatment with CPT and MMC, respectively. Untreated cells were included as controls. Claspin NT-KR levels in the chromatin-bound fraction are diminished in response to CPT, but not MMC.

(B) WT and V26A DT40 cells were incubated with CPT (100 nM) for 1 hr or MMC (150 nM) for 6 hr. Lysates were fractionated into cytoplasmic and nuclear soluble (S1 + S3) or chromatin-bound (P3) fractions and immunoblotted with the indicated antibodies. SCC1 and MEK2 serve as controls for loading and the effectiveness of fractionation. "C" and "M" indicate treatment with CPT and MMC, respectively. Untreated cells were included as controls. Claspin levels in the chromatin-bound fraction of V26A cells are diminished in response to CPT, but not MMC.

(C) WT and V26A DT40 cells were treated with CPT (100 nM) for 1 hr or MMC (150 nM) for 6 hr. Whole-cell extracts were immunoblotted with the indicated antibodies. Untreated cells are included as controls. "C" and "M" indicate treatment with CPT and MMC, respectively. Ser345 phosphorylation of CHK1 is impaired in V26A cells only in response to CPT.

(D) We propose that genotoxic lesions generated by CPT (upper panel, left) require BRCA1/BARD1 E3 ligase activity, which ubiquitylates claspin to promote CHK1 phosphorylation (pCHK1, center) and homology-directed repair. Lesions such as those generated by MMC bypass this pathway (upper panel, right), separating BRCA1 E3-independent from -dependent DNA damage responses. The E3 ligase-inactive BRCA1 V26A mutant is therefore defective for the response to CPT, but not MMC (lower panel). See also Figure S4.

claspin ubiquitylation affects its accumulation on chromatin. To do this, we compared the levels of WT or NT-KR mutant claspin in the soluble (S1+S3) or chromatin-bound (P3) fractions of nuclear extracts prepared from 293T cells exposed to these agents (Figure 4A). WT claspin is detected in both the soluble and chromatin-bound protein fractions of nuclear extracts. In contrast, NT-KR mutant claspin does not accumulate in the chromatin-bound protein fraction in cells exposed to CPT. Indeed, a similar difference is observed when the levels of claspin were measured in WT or V26A cells treated with CPT or MMC (Figure 4B). Claspin levels in the soluble fraction are similar in both cell types, before (−) and after exposure to CPT or MMC, with a slight reduction in V26A cells exposed to CPT (compare lanes 2 and 3 with 5 and 6 in row 1). In the chromatin-bound fraction, claspin expression in untreated V26A cells, or even in V26A cells exposed to MMC, is similar to the levels found in WT cells. Remarkably, however, in the chromatin-bound protein fraction prepared from V26A cells exposed to CPT, claspin is specifically diminished in comparison to WT controls (compare lanes 2, 5, in row 4). Interestingly, the diminution in chromatin-bound claspin after CPT exposure is not accompanied by a reduction in its retention time measured by fluorescence recovery after photobleaching (FRAP, Figures S2A–S2C). Instead, we observe a reduction in the half-life of NT-KR mutant claspin relative to the WT (Figures S2D and S2E). Together, these results suggest that ubiquitylation of claspin by BRCA1/BARD1 is required for its accumulation in the chromatin-bound protein fraction in response to CPT and may exert this effect via the control of protein stability.

We therefore analyzed the effect on DNA-damage signaling of decreased chromatin-bound claspin levels in V26A cells exposed to CPT. We first investigated the steps leading to activation of the ataxia and Rad3-like (ATR) kinase, because claspin is known to coactivate CHK1 in an ATR-dependent manner [9, 20]. We find that the phosphorylation of MCM2 at Ser108, a known target for ATR phosphorylation after DNA damage [24], is induced above predamage levels after the exposure of WT cells to CPT or MMC (Figure 4C, lanes 2 and 3). MCM2 S108 phosphorylation was elevated even in undamaged

V26A cells and was not greatly increased after CPT or MMC exposure. This may reflect that endogenously arising DNA lesions in dividing V26A cells (marked by the increased basal level of SCE formation (Table S1; Figure 1F) constitutively elevate the resting level of ATR-dependent checkpoint activation. Nevertheless, these findings suggest that BRCA1 E3 inactivation does not prevent ATR-activated phosphorylation of MCM2 per se.

In contrast, the phosphorylation of CHK1, an evolutionarily conserved and essential component of the machinery for checkpoint enforcement and DNA repair by HDR [10, 13], is selectively compromised after CPT exposure by the V26A mutation in BRCA1. ATR phosphorylates CHK1 on residues Ser317 and Ser345 [10, 25]. These modifications accompany and are essential for CHK1 activation mediated by ATR [10, 25] and are therefore used as surrogate markers for this event [25]. Although MMC triggers CHK1 modification on Ser345 in V26A as well as WT cells (Figure 4C, lanes 3 and 6), phosphorylation of this Ser residue is selectively impaired in V26A cells after exposure to CPT (compare lanes 2 and 5). Thus collectively, our observations indicate that inactivation of the E3 ligase activity of BRCA1 causes a specific failure in signal transmission from ATR to CHK1 in response to CPT, but not MMC.

CHK1 activation triggered by DNA damage occurs on chromatin [8]. Claspin forms a trimolecular complex with BRCA1 and CHK1 that is essential for CHK1 activation [9], and its turnover is reported to regulate CHK1 activation during recovery from damage-induced G2 arrest [26, 27]. In this light, our findings suggest a mechanism (Figure 4D) wherein ubiquitin conjugation to claspin by the BRCA1 E3 ligase promotes efficient CHK1 activation by maintaining chromatin-bound claspin levels after replication blockage triggered by CPT but not MMC. In turn, activated CHK1 mediates checkpoint enforcement [10] as well as DNA repair by homologous recombination, through modulation of the interaction between BRCA2 and the recombinase, RAD51 [12, 13]. Thus, our results suggest a novel role for claspin ubiquitylation by BRCA1 E3 ligase activity in selectively promoting the homology-directed repair of a subset of genotoxic lesions.

Why the claspin-CHK1 axis should require BRCA1 E3 ligase activity in response to CPT but not MMC is presently unclear. CPT traps a reversible, cleavable DNA structure by inhibiting the religation step during topoisomerase I-catalyzed reactions [28]; the reversible complex is then converted into irreversible strand breaks upon encounter with the machinery for DNA replication. MMC triggers intrastrand lesions as well as DNA crosslinks, which block DNA replication forks; strand breakage accompanies their repair [18]. Thus, both genotoxins induce lesions that block DNA replication and whose repair by homologous recombination involves strand-break intermediates. However, there is insufficient knowledge to speculate what may distinguish these lesions or repair intermediates structurally to explain the differential requirement for BRCA1 activity in their resolution. Intriguingly, we find that V26A mutant cells are selectively more sensitive than their WT counterparts to the effect of several drugs that inhibit topoisomerase I (CPT, SN38) as well as topoisomerase II (doxorubicin, etoposide), but not to MMC (Figures S3A–S3E). Moreover, V26A mutant cells fail to activate CHK1 Ser345 phosphorylation in response to topoisomerase inhibitors at doses that suffice to evoke this response in WT cells (Figure S3F), further supporting the notion that BRCA1 E3 ligase activity is required for CHK1 activation in response to a subset of genotoxic lesions.

Our demonstration that BRCA1 E3 ligase activity is required for the response to some, but not all, genotoxic lesions provides new functional insight apposite to recent work concerning BRCA1's biological role. Recent reports suggest that the murine BRCA1 point mutation I26A, functionally analogous to the avian V26A mutation used here, neither affects ionizing radiation sensitivity, nor the repair of endonuclease-induced DNA breaks by homologous recombination [5]. Furthermore, mice harboring this mutation do not develop breast cancers [6]. However, a different BRCA1 point mutation that abolishes both E3 ligase activity and BARD1 binding potentiates cellular sensitivity to poly-ADP ribose polymerase (PARP) inhibition and cisplatin, and mice carrying this mutation do develop breast cancer [29]. Notably, at least some of the BRCA1 missense mutations found in familial breast cancer patients abolish E3 ligase activity without impairing BARD1 binding [4], like the V26A mutation used in our work, but in contrast to the murine I26A mutation. Moreover, we find that overexpression of the NT-KR mutant of claspin in human cells depleted of the endogenous WT protein by RNAi has a modest effect on CPT sensitivity but does not affect sensitivity to MMC (Figures S4A–S4C), consistent with the results reported here. Thus, in light of the possible differences between model systems and species, further exploration of the selective requirement for BRCA1 E3 activity in the response to certain forms of DNA damage that we have identified in this work seems warranted.

Our observations, if confirmed in human cancer cells, could have potential implications for the treatment of BRCA1-deficient familial cancers in which mutations selectively impair E3 ligase activity without creating a nullizygous phenotype [4]. Our findings suggest that there may be benefit in such a setting from treatment with CPT but not MMC. We speculate that this may also apply to some of the ~10% of sporadic cancers belonging to the basal-like group, which exhibit certain phenotypic characteristics suggestive of impaired but not absent BRCA1 deficiency [30, 31]. These hypotheses warrant further investigation.

Experimental Procedures

Cell Culture

293T cells were cultured in Dulbecco's modified Eagle medium supplemented with 10% fetal bovine serum and 1% antibiotic-antimycotic agent at 37°C. DT40 cells were maintained in RPMI-1640 medium (GIBCO-BRL) supplemented with 10^{-5} M β-mercaptoethanol, 10% fetal calf serum (FCS), 1% antibiotic-antimycotic agent, and 5% chicken serum (GIBCO-BRL) at 39°C.

Plasmids

cDNA of *Gg*BRCA1 (1–222) and *Gg*BARD1 (1–159) were amplified by PCR from a cDNA pool generated with SuperScript® III First-Strand Synthesis System (Invitrogen) with Pfx DNA polymerase (Invitrogen) and subcloned into p3X-FLAG-CMV or pcDNA3-myc vectors. For the purification of *Gg*BRCA1 (1–300), cDNA was amplified by PCR as above and subcloned into pGEX-4T3 vector in frame with FLAG amino-terminal tag. For cDNA of *Gg*BRCA1 V26A, both 1–222 and 1–300, were obtained from the cDNA pool derived from V26A cells with same method outlined above. Myc-tagged *Hs*BRCA1(1–772), *Hs*BARD1, His-tagged *Hs*BARD1, and HA-tagged-*Hs*Ubiquitin were described previously [32]. cDNA of *Hs*claspin was purchased from Geneservice and PCR was performed to ligate into p3XFLAG-CMV or pcDNA3.1-Hygro (in frame with NH2-terminal EGFP tag) vectors. The missense mutant of claspin (NT-KR) was generated by site-directed mutagenesis. Truncation mutant of claspin (1–331) was generated by introducing an in-frame NotI or BamHI site and a stop codon in the appropriate position by site-directed mutagenesis followed by digestion with either NotI or BamHI to remove the fragment.

Gene Targeting

The sequences of the oligonucleotide primers used here are in Supplemental Experimental Procedures. The homologous sequences of avian BRCA1 used for targeting were isolated by PCR from DT40 genomic DNA using primers LA F1, LA R1 for left homology arm and RA F1, RA R1 for right homology arm and cloned into a targeting vector bearing either a neomycin or blasticidin resistant cassette. The V26A mutation and BsrDI diagnostic (silent mutation) restriction site were generated by site-directed mutagenesis using the Quickchange Site-Directed Mutagenesis Kit (Stratagene). Heterozygous cells were subjected to a second round of targeting and homozygous mutant cells were screened by PCR using primer DV26A and LAR1 (Figure 2A) followed by digestion with BsrDI.

Antibodies

The rabbit polyclonal anti-*Gg*BRCA1 antibodies were raised against the recombinantly expressed N-terminal 300 amino acids of avian BRCA1 protein. Anti-*Gg*claspin antibody was generously provided by Dr. David Gillespie (Beatson Institute for Cancer Research, Glasgow). Other antibodies used in this study were as follows: anti-FLAG (M2) and anti-β-actin (AC-15) antibodies (Sigma); anti-Myc (9E10), anti-ATR (N-19), and anti-CHK1 (G-4) antibodies (Santa Cruz Biotechnology); anti-phospho-ATM (S1981) and anti-phospho-CHK1 (S345) (Cell Signaling Technology); anti-RAD51 (Ab-1) (Calbiochem); and anti-HA (12CA5) (Roche). All western blotting or immunofluorescence reagents were used at the dilutions recommended by the manufacturers.

Drug Sensitivity Assay

Cells were plated into 96-well plates at a density of 8,000 cells per well. Different doses of mitomycin C (Sigma) and camptothecin (Sigma) were added, and the plates were incubated at 39°C for 40 hr. Cell Titer-Blue reagents (Promega) were added to each well of the 96-well plate according to the manufacturer's guidelines. The plates were incubated at 37°C for approximately 1–2 hr in a humidified 5% CO_2 atmosphere. The intensity of Titer-Blue signal, and thus a fraction of viable cells per well was determined using the Fusion Plate Reader (Perkin Elmer/Packard) at A590 nm. Each experiment was done in quadruplicate.

Western Blots and Immunoprecipitation

293T cells were transfected by a standard calcium chloride method. Thirty-six hr after transfection, cells were lysed with 0.5% NP-40 lysis buffer (50 mM Tris-HCl pH 7.5, 150 mM NaCl, 0.5% NP-40, 50 mM NaF, 1 mM DTT, 1 mM Na_3VO_4, complete protease inhibitor cocktail [Roche], and 1 mM PMSF). To detect ubiquitylation in vivo, we lysed cells with 1% SDS lysis buffer (1% SDS, 0.5 mM EDTA, 1 mM DTT and 50 mM Tris HCl pH 7.5) at 100°C for 10 min. After collecting supernatant, the lysate was diluted 10 times in NP40 lysis buffer for immunoprecipitation. Immunoprecipitates were washed extensively in NP-40 lysis buffer and resolved by SDS-PAGE. For fractionation, cells were lysed with buffer A (10 mM HEPES pH 7.9, 10 mM KCl, 1.5 mM $MgCl_2$, 0.034 M sucrose, 10% glycerol, 1 mM DTT, 100 μM PMSF, complete protease inhibitor cocktail [Roche], 5 mM Na_3VO_4, 10 mM NaF, 1 μM Okadaic acid) with 0.1% Triton X-100 for 5 min on ice. Cells were centrifuged at 1300 × g for 4 min and supernatant collected (S1). S1 was further clarified by high speed centrifugation. The nuclei (P1) were washed in buffer A, then lysed by buffer B (3 mM EDTA, 0.2 mM EGTA, 1 mM DTT, PMSF, complete protease inhibitor cocktail [Roche], 5 mM Na_3VO_4, 10 mM NaF, 1 μM Okadaic acid) for 1 min on ice. Nuclei were centrifuged at 1,700 × g for 4 min. Soluble nuclear fraction (S3) was collected. The insoluble chromatin pellet was then resuspended in buffer A with 1 mM $CaCl_2$ and 0.2 U micrococcal nuclease, incubated at 37°C for 10 min. Chromatin fraction (P3) was collected by high speed centrifugation.

Immunofluorescence Microscopy

To detect RAD51 foci, we spun cells onto glass slides by using a cytocentrifuge (Shandon). After drying for 5 min, cells were fixed with 4% paraformaldehyde for 10 min at room temperature. Samples were solubilized with 0.2% Triton X-100 for 5 min and blocked with 3% BSA in 1xPBS, 0.1% Tween-20, 0.1%Triton X-100 (PBST) for 15 min. Cells were then probed with a rabbit polyclonal anti-RAD51 antibody diluted 1:1,000 for 30 min.

Sister Chromatid Exchange Assay

The sister chromatid exchange assay was performed as described previously [33]. Briefly, cells were cultured for two cell cycles in the presence of 10 μM bromodeoxyuridine and with or without 10 nM camptothecin (CPT) and 150 nM mitomycin C (MMC) for the second cell cycle. Cells were pulsed with 100 ng/ml colcemid for 3 hr before harvest. Cells were hypotonically swollen in 75 mM KCl for 20 min at room temperature before fixation in freshly prepared Carnoy's solution (methanol: acetic acid, 3:1) for 30 min at room temperature. Fixed cells were dropped onto slides, dried at 50°C for 20 min and then incubated for 20 min in 10 μg/ml Hoescht-33258 (Sigma), diluted in 0.05 M sodium phosphate buffer, pH 6.8 at room temperature. Slides were irradiated with UV-A (365 nm) for 90 min and then incubated in prewarmed 2X SSC for 1 hr at 62°C. Slides were stained with freshly prepared Leishman's stain (Sigma) (diluted 1:3 in 0.05 M sodium phosphate buffer, pH 6.8) for 2 min. Slides were dried and mounted with Eukitt Mounting Media (Electron Microscopy Sciences) under a coverslip. Cells in metaphase were visualized with a 100X objective on a Zeiss Axioskop 2 microscope and 50 spreads scored blind to the observer.

Protein Purification

GST-FLAG-*Gg*BRCA1 (1–300, WT, and V26A) and GST-FLAG-claspin 1–331 were purified from BL21/DE3 bacterial cells following isopropyl-L-thio-B-D-galactopyranoside (IPTG) induction as previously described [32]. Purification of His-UbcH5c and His- BARD1 was previously described [32]. Purification of His-BRCA11-304 and His-BARD11-320 as a RING heterodimer was performed as previously described [32]. Rabbit E1 (Affiniti) and mammalian ubiquitin (Affiniti) were purchased commercially.

Ubiquitin Ligation Assay In Vitro

The procedure used for the in vitro ubiquitin ligation assay was performed as previously described [32] with a reaction mixture (30 AL) that contained 50 mmol/L Tris-HCl (pH 7.5), 5 mmol/L $MgCl_2$, 2 mmol/L ATP, 0.6 mmol/L DTT, 1 μg mammalian ubiquitin, 40 ng E1, 0.3 μg UbcH5c, 1 μg His-BRCA11-304/His-BARD11-320, and 1 μg of GST-FLAG-claspin 1–331. The ubiquitylation products were detected by immunoblotting with the indicated antibodies.

Preparation of Samples for Liquid Chromatography-Tandem Mass Spectrometry

After in vitro ubiquitin ligation, samples were resolved by SDS-PAGE. Gels were silver stained and excised spots were enzymatically cleaved in gel as previously described [34]. Each spot was reduced with 10 mM DTT at 56°C for 30 min and alkylated with 50 mM iodoacetamide (Sigma, Buchs, Switzerland) in the dark for 30 min followed by enzymatic cleavage with 2 μg Trypsin (Promega).

LC-MS/MS Analysis

The samples were analyzed on a LTQ Orbitrap XL mass spectrometer (MS; Thermo-Fisher Scientific, Bremen, Germany), which was connected online to a nanoelectrospray ion source (Thermo-Fisher Scientific, Bremen, Germany). Peptide separation was carried out using an Eksigent Tempo nano LC 1D+ System (Eksigent Technologies, Dublin, CA, USA) equipped with a RP-HPLC column (75 μm × 15 cm) packed in-house with C18 resin (Magic C18 AQ 3 μm; Michrom BioResources, Auburn, CA, USA) using a linear gradient from 96% solvent A (0.15% formic acid, 2% acetonitrile) and 4% solvent B (0.15% formic acid, 98% acetonitrile) to 25% solvent B over 40 min at a flow rate of 0.3 μl/min. We injected 4 μl of each sample per liquid chromatography-tandem mass spectrometry (LC-MS/MS) run for analysis. After every two samples, a peptide mixture containing 200 fmol of [Glu1]-Fibrinopeptide B human (Sigma, Buchs, Switzerland) was analyzed by LC-MS/MS to constantly monitor the performance of the LC-MS/MS system.

Acquired MS2 scans were searched against the UniProtKB/Swiss-Prot protein database (release v56.9) using the Sorcerer-SEQUEST® v4.0.4 search algorithm, which was run on the SageN Sorcerer (Thermo Electron). In silico trypsin, digestion was performed after lysine and arginine (unless followed by proline) tolerating two missed cleavages in fully tryptic peptides. Allowed monoisotopic mass error for the precursor ions was 50 ppm. A fixed residue modification parameter was set for carboxyamidomethylation (+57.021464 Da) of cysteine residues. Oxidation of methionine (+15.99492 Da) and ubiquitylation (+114.042923 Da) of lysine residues were set as variable residue modification parameter. For scoring, a maximum of two missed cleavages were considered. Search results were evaluated on the Trans Proteomic Pipeline (TPP v4.02).

Supplemental Information

Supplemental Information includes four figures, two tables, and Supplemental Experimental Procedures and can be found with this article online at http://dx.doi.org/10.1016/j.cub.2012.07.034.

Acknowledgments

We thank David Gillespie (Glasgow) for providing anti-*Gg*claspin antibody and members of our group for helpful discussion and criticism. This work was funded in A.R.V.'s laboratory by the UK Medical Research Council.

Received: March 27, 2012
Revised: June 9, 2012
Accepted: July 6, 2012
Published online: August 2, 2012

References

1. Venkitaraman, A.R. (2002). Cancer susceptibility and the functions of BRCA1 and BRCA2. Cell *108*, 171–182.
2. Brzovic, P.S., Keeffe, J.R., Nishikawa, H., Miyamoto, K., Fox, D., 3rd, Fukuda, M., Ohta, T., and Klevit, R. (2003). Binding and recognition in the assembly of an active BRCA1/BARD1 ubiquitin-ligase complex. Proc. Natl. Acad. Sci. USA *100*, 5646–5651.
3. Hashizume, R., Fukuda, M., Maeda, I., Nishikawa, H., Oyake, D., Yabuki, Y., Ogata, H., and Ohta, T. (2001). The RING heterodimer BRCA1-BARD1 is a ubiquitin ligase inactivated by a breast cancer-derived mutation. J. Biol. Chem. *276*, 14537–14540.
4. Morris, J.R., Pangon, L., Boutell, C., Katagiri, T., Keep, N.H., and Solomon, E. (2006). Genetic analysis of BRCA1 ubiquitin ligase activity and its relationship to breast cancer susceptibility. Hum. Mol. Genet. *15*, 599–606.
5. Reid, L.J., Shakya, R., Modi, A.P., Lokshin, M., Cheng, J.T., Jasin, M., Baer, R., and Ludwig, T. (2008). E3 ligase activity of BRCA1 is not essential for mammalian cell viability or homology-directed repair of double-strand DNA breaks. Proc. Natl. Acad. Sci. USA *105*, 20876–20881.
6. Shakya, R., Reid, L.J., Reczek, C.R., Cole, F., Egli, D., Lin, C.S., deRooij, D.G., Hirsch, S., Ravi, K., Hicks, J.B., et al. (2011). BRCA1 tumor suppression depends on BRCT phosphoprotein binding, but not its E3 ligase activity. Science *334*, 525–528.
7. Zhu, Q., Pao, G.M., Huynh, A.M., Suh, H., Tonnu, N., Nederlof, P.M., Gage, F.H., and Verma, I.M. (2011). BRCA1 tumour suppression occurs via heterochromatin-mediated silencing. Nature *477*, 179–184.
8. Smits, V.A., Reaper, P.M., and Jackson, S.P. (2006). Rapid PIKK-dependent release of Chk1 from chromatin promotes the DNA-damage checkpoint response. Curr. Biol. *16*, 150–159.
9. Lin, S.Y., Li, K., Stewart, G.S., and Elledge, S.J. (2004). Human Claspin works with BRCA1 to both positively and negatively regulate cell proliferation. Proc. Natl. Acad. Sci. USA *101*, 6484–6489.
10. Liu, Q., Guntuku, S., Cui, X.S., Matsuoka, S., Cortez, D., Tamai, K., Luo, G., Carattini-Rivera, S., DeMayo, F., Bradley, A., et al. (2000). Chk1 is an essential kinase that is regulated by Atr and required for the G(2)/M DNA damage checkpoint. Genes Dev. *14*, 1448–1459.
11. Yarden, R.I., Pardo-Reoyo, S., Sgagias, M., Cowan, K.H., and Brody, L.C. (2002). BRCA1 regulates the G2/M checkpoint by activating Chk1 kinase upon DNA damage. Nat. Genet. *30*, 285–289.
12. Bahassi, E.M., Ovesen, J.L., Riesenberg, A.L., Bernstein, W.Z., Hasty, P.E., and Stambrook, P.J. (2008). The checkpoint kinases Chk1 and Chk2 regulate the functional associations between hBRCA2 and Rad51 in response to DNA damage. Oncogene *27*, 3977–3985.
13. Sørensen, C.S., Hansen, L.T., Dziegielewski, J., Syljuåsen, R.G., Lundin, C., Bartek, J., and Helleday, T. (2005). The cell-cycle checkpoint kinase Chk1 is required for mammalian homologous recombination repair. Nat. Cell Biol. *7*, 195–201.
14. Martin, R.W., Orelli, B.J., Yamazoe, M., Minn, A.J., Takeda, S., and Bishop, D.K. (2007). RAD51 up-regulation bypasses BRCA1 function and is a common feature of BRCA1-deficient breast tumors. Cancer Res. *67*, 9658–9665.
15. Vandenberg, C.J., Gergely, F., Ong, C.Y., Pace, P., Mallery, D.L., Hiom, K., and Patel, K.J. (2003). BRCA1-independent ubiquitination of FANCD2. Mol. Cell *12*, 247–254.
16. Yamazoe, M., Sonoda, E., Hochegger, H., and Takeda, S. (2004). Reverse genetic studies of the DNA damage response in the chicken B lymphocyte line DT40. DNA Repair (Amst.) *3*, 1175–1185.
17. Furuta, T., Hayward, R.L., Meng, L.H., Takemura, H., Aune, G.J., Bonner, W.M., Aladjem, M.I., Kohn, K.W., and Pommier, Y. (2006). p21CDKN1A allows the repair of replication-mediated DNA double-strand breaks induced by topoisomerase I and is inactivated by the checkpoint kinase inhibitor 7-hydroxystaurosporine. Oncogene *25*, 2839–2849.
18. Bae, J.B., Mukhopadhyay, S.S., Liu, L., Zhang, N., Tan, J., Akhter, S., Liu, X., Shen, X., Li, L., and Legerski, R.J. (2008). Snm1B/Apollo mediates replication fork collapse and S Phase checkpoint activation in response to DNA interstrand cross-links. Oncogene *27*, 5045–5056.
19. Sonoda, E., Sasaki, M.S., Morrison, C., Yamaguchi-Iwai, Y., Takata, M., and Takeda, S. (1999). Sister chromatid exchanges are mediated by homologous recombination in vertebrate cells. Mol. Cell. Biol. *19*, 5166–5169.
20. Kumagai, A., and Dunphy, W.G. (2000). Claspin, a novel protein required for the activation of Chk1 during a DNA replication checkpoint response in Xenopus egg extracts. Mol. Cell *6*, 839–849.
21. Lee, J., Gold, D.A., Shevchenko, A., Shevchenko, A., and Dunphy, W.G. (2005). Roles of replication fork-interacting and Chk1-activating domains from Claspin in a DNA replication checkpoint response. Mol. Biol. Cell *16*, 5269–5282.
22. Wu, W., Koike, A., Takeshita, T., and Ohta, T. (2008). The ubiquitin E3 ligase activity of BRCA1 and its biological functions. Cell Div. *3*, 1.
23. Nishikawa, H., Ooka, S., Sato, K., Arima, K., Okamoto, J., Klevit, R.E., Fukuda, M., and Ohta, T. (2004). Mass spectrometric and mutational analyses reveal Lys-6-linked polyubiquitin chains catalyzed by BRCA1-BARD1 ubiquitin ligase. J. Biol. Chem. *279*, 3916–3924.
24. Cortez, D., Glick, G., and Elledge, S.J. (2004). Minichromosome maintenance proteins are direct targets of the ATM and ATR checkpoint kinases. Proc. Natl. Acad. Sci. USA *101*, 10078–10083.
25. Zhao, H., and Piwnica-Worms, H. (2001). ATR-mediated checkpoint pathways regulate phosphorylation and activation of human Chk1. Mol. Cell. Biol. *21*, 4129–4139.
26. Mailand, N., Bekker-Jensen, S., Bartek, J., and Lukas, J. (2006). Destruction of Claspin by SCFbetaTrCP restrains Chk1 activation and facilitates recovery from genotoxic stress. Mol. Cell *23*, 307–318.
27. Peschiaroli, A., Dorrello, N.V., Guardavaccaro, D., Venere, M., Halazonetis, T., Sherman, N.E., and Pagano, M. (2006). SCFbetaTrCP-mediated degradation of Claspin regulates recovery from the DNA replication checkpoint response. Mol. Cell *23*, 319–329.
28. Liu, L.F. (1989). DNA topoisomerase poisons as antitumor drugs. Annu. Rev. Biochem. *58*, 351–375.
29. Drost, R., Bouwman, P., Rottenberg, S., Boon, U., Schut, E., Klarenbeek, S., Klijn, C., van der Heijden, I., van der Gulden, H., Wientjens, E., et al. (2011). BRCA1 RING function is essential for tumor suppression but dispensable for therapy resistance. Cancer Cell *20*, 797–809.
30. Turner, N.C., and Reis-Filho, J.S. (2006). Basal-like breast cancer and the BRCA1 phenotype. Oncogene *25*, 5846–5853.
31. Shakya, R., Szabolcs, M., McCarthy, E., Ospina, E., Basso, K., Nandula, S., Murty, V., Baer, R., and Ludwig, T. (2008). The basal-like mammary carcinomas induced by Brca1 or Bard1 inactivation implicate the BRCA1/BARD1 heterodimer in tumor suppression. Proc. Natl. Acad. Sci. USA *105*, 7040–7045.
32. Nishikawa, H., Wu, W., Koike, A., Kojima, R., Gomi, H., Fukuda, M., and Ohta, T. (2009). BRCA1-associated protein 1 interferes with BRCA1/BARD1 RING heterodimer activity. Cancer Res. *69*, 111–119.
33. Niedzwiedz, W., Mosedale, G., Johnson, M., Ong, C.Y., Pace, P., and Patel, K.J. (2004). The Fanconi anaemia gene FANCC promotes homologous recombination and error-prone DNA repair. Mol. Cell *15*, 607–620.
34. Keller, A., Eng, J., Zhang, N., Li, X.J., and Aebersold, R. (2005). A uniform proteomics MS/MS analysis platform utilizing open XML file formats. Mol. Syst. Biol. *1*, 1–8.

Published OnlineFirst August 3, 2012; DOI:10.1158/0008-5472.CAN-12-1057

Cancer Research

RNF8 Regulates Assembly of RAD51 at DNA Double-Strand Breaks in the Absence of BRCA1 and 53BP1

Shinichiro Nakada[1,2], Rikako Miyamoto Yonamine[2], and Koichi Matsuo[2,3]

Abstract

The tumor suppressor protein BRCA1 localizes to sites of DNA double-strand breaks (DSB), promoting repair by homologous recombination through the recruitment of DNA damage repair proteins. In normal cells, homologous recombination largely depends on BRCA1. However, assembly of the pivotal homologous recombination regulator RAD51 can occur independently of BRCA1 in the absence of 53BP1, another DNA damage response protein. How this assembly process proceeds is unclear, but important to understand in tumor cell settings where BRCA1 is disabled. Here we report that RNF8 regulates BRCA1-independent homologous recombination in 53BP1-depleted cells. RNF8 depletion suppressed the recruitment of RAD51 to DSB sites without affecting assembly or phosphorylation of the replication protein RPA in neocarzinostatin-treated or X-ray-irradiated BRCA1/53BP1-depleted cells. Furthermore, RNF8/BRCA1/53BP1-depleted cells exhibited less efficient homologous recombination than BRCA1/53BP1-depleted cells. Intriguingly, neither RNF8 nor its relative RNF168 were required for RAD51 assembly at DSB sites in 53BP1-expressing cells. Moreover, RNF8-independent RAD51 assembly was found to be regulated by BRCA1. Together, our findings indicate a tripartite regulation of homologous recombination by RNF8, BRCA1, and 53BP1. In addition, our results predict that RNF8 inhibition may be a useful treatment of BRCA1-mutated/53BP1^{low} cancers, which are considered resistant to treatment by PARP1 inhibitors and of marked current clinical interest. *Cancer Res; 72(19); 4974–83. ©2012 AACR.*

Introduction

DNA double-strand breaks (DSB) are repaired by 2 major systems: nonhomologous end joining (NHEJ) and homologous recombination. NHEJ is an intrinsically error prone repair system that operates throughout the cell cycle. Homologous recombination is an error-free repair system, but it is limited to the late S and G_2 phases because the replicated DNA strand is used as a template (1). Homologous recombination is initiated by nucleolytic degradation of the DSB ends to generate a 3′ single-stranded DNA (ssDNA) overhang (2, 3). The resultant ssDNA is immediately coated by replication protein A (RPA). Breast cancer, early onset 2 (BRCA2) then promotes the displacement of RPA from the ssDNA by RAD51 to form a RAD51-ssDNA filament. RAD51 searches for homologous DNA sequences in a sister chromatid and promotes DNA strand invasion. The homologous DNA sequence then serves as template for the synthesis of new DNA. During homologous recombination, BRCA1 is also recruited to DSBs, where it promotes efficient RAD51 alignment (2). In addition to DSB repair, homologous recombination is also required for the repair of spontaneous DNA breaks, and defective homologous recombination induces severe genomic instability. Germline mutations in the *BRCA1* or *BRCA2* genes increase the risk of early-onset breast and ovarian cancers (2, 4). Because patient tumor cells often possess 2 mutant alleles of *BRCA1* or *BRCA2* and show defective homologous recombination, inactivation of either BRCA1- or BRCA2-dependent homologous recombination is thought to trigger tumorigenesis.

Upon DNA DSB introduction, the following processes occur: the histone H2AX is phosphorylated by ataxia telangiectasia mutated (ATM); the mediator of DNA damage checkpoint 1 (MDC1) binds to the phosphorylated H2AX (γH2AX); and ATM phosphorylates MDC1 at the region surrounding the DSB. The E3 ubiquitin ligase really interesting new gene (RING) finger protein 8 (RNF8) binds to phosphorylated MDC1 at DSB sites and promotes the recruitment of another E3 ubiquitin ligase, RNF168. RNF8 and RNF168 conjugate Lys 63-linked ubiquitin chains onto histone H2A with their cognate E2 ubiquitin-conjugating enzyme UBC13 and induce chromatin remodeling (5–11). Recent studies showed that RNF8 and RNF168 also ubiquitinate non-histone substrates, which are also important for DSB signaling (12–15). UBC13-RNF8/RNF168-dependent ubiquitination promotes the recruitment of BRCA1 and p53-binding protein 1 (53BP1), another DNA damage response factor that is recruited to DSBs (6–14, 16; Supplementary Fig S1). A large proportion of the BRCA1 that localizes to DSB sites is a component of the BRCA1-A complex, consisting of a

Authors' Affiliations: [1]Department of Bioregulation and Cellular Response, Graduate School of Medicine, Osaka University, Osaka, Japan; [2]Center of Integrated Medical Research, and [3]Laboratory of Cell and Tissue Biology, School of Medicine, Keio University, Tokyo, Japan

Note: Supplementary data for this article are available at Cancer Research Online (http://cancerres.aacrjournals.org/).

Corresponding Author: Shinichiro Nakada, Department of Bioregulation and Cellular Response, Graduate School of Medicine, Osaka University, 2-2 Yamadaoka, Suita-shi, Osaka 565-0871, Japan. Phone: 81-6-6879-3398; Fax: 81-6-6879-3096;E-mail: snakada.res@gmail.com.

doi: 10.1158/0008-5472.CAN-12-1057

Published OnlineFirst August 3, 2012; DOI:10.1158/0008-5472.CAN-12-1057

BRCA1/BARD1 heterodimer, the ubiquitin interacting motif (UIM)-containing protein RAP80, deubiquitinating enzyme BRCC36, an adaptor protein ABRAXAS, BRCC45, and MERIT40 (2, 5–11, 17–19). RAP80 interacts with the Lys 63-linked chain that is generated by UBC13-RNF8/RNF168 and brings BRCA1 to DSB sites (2, 5–11, 17–20; Supplementary Fig S1A). This complex does not directly interact with the DSB ends and does not promote homologous recombination (21, 22). A small subset of BRCA1 forms protein complexes with homologous recombination factors such as BACH1, TopBP1, CtIP, MRE11, RAD50, NBS1, and RAD51, localizes to DSB sites independently of RAP80 and promotes DNA end resection, RAD51 assembly, and homologous recombination (2, 21, 22; Supplementary Fig. S1A and S1B). Chicken UBC13-knockout DT40 cells show defective RAD51 assembly at DSB sites and inefficient homologous recombination (5). Moreover, the overexpression of the deubiquitinating enzyme OTU domain, ubiquitin aldehyde binding 1 (OTUB1), which suppresses DNA damage-dependent chromatin ubiquitination through noncatalytic inhibition of UBC13 activity, suppresses homologous recombination (23). These data strongly suggest that DNA damage-dependent ubiquitination is crucial for homologous recombination. However, it is not known whether UBC13-RNF8/RNF168-dependent ubiquitination is required for homologous recombination and the RAP80-independent recruitment of BRCA1.

Cells have multiple DNA repair systems other than homologous recombination. These systems work redundantly, each operating to repair DNA in the event that other repair systems are ineffective. PARP1 is required for efficient single-strand break repair and has a role at stalled replication forks (4). When PARP1 is pharmacologically inhibited, DNA damage is repaired through homologous recombination in normal cells. In contrast, homologous recombination-defective cells, such as BRCA1- or BRCA2-negative breast cancer cells, are intrinsically sensitive to PARP1 inhibitors. Therefore, PARP1 inhibition induces synthetic lethality in BRCA1- or BRCA2- negative cancer cells with mild side effects, and this synthetic lethality is exploited in the clinical setting (4). However, a recent study predicts that some of BRCA1-negative cancer cells are resistant to PARP1 inhibition. This study revealed that *BRCA1* mutations and low-53BP1 expression are correlated with poor patient prognosis (24). In an experimental setting, loss of *53BP1* restores homologous recombination in BRCA1-deficient murine cells and renders them insensitive to PARP1 inhibitors. (24, 25; Supplementary Fig. S1C). These data suggest the existence of a molecule that regulates BRCA1-independent homologous recombination in the absence of 53BP1, and if such a model exists, the molecule regulating BRCA1-independent homologous recombination may be a therapeutic target for the treatment of cancer cells with *BRCA1* mutation and low-53BP1 expression.

In this study, we analyzed the role of RNF8 in RAD51 assembly at DSB sites and the subsequent homologous recombination. Depletion of RNF8 or RNF168 did not affect the RAD51 assembly at DSB sites after X-ray irradiation. This RNF8-independent RAD51 assembly was abolished by BRCA1 depletion. In contrast, depletion of either RNF8 or RNF168 strongly suppressed RAD51 assembly in BRCA1/53BP1-depleted cells. Furthermore, homologous recombination, as measured by a direct repeat GFP (DR-GFP) reporter (26) was also significantly suppressed in RNF8/BRCA1/53BP1-depleted cells, although BRCA1/53BP1-depleted cells showed a normal level of homologous recombination efficiency. Our data indicate that RAD51-dependent homologous recombination is regulated by RNF8, RNF168, BRCA1, and 53BP1. Our findings also suggest that inhibition of the activity of RNF8 or RNF168 can suppress BRCA1-independent homologous recombination in 53BP1^{low} tumor cells.

Materials and Methods

Cell culture

HCT116 human colon carcinoma cells, HeLa cells, RNF8$^{-/-}$ mouse embryonic fibroblasts (MEF) and wild type (WT) MEFs were grown in Dulbecco's Modified Eagle's Medium with 10% FBS. U2OS human osteosarcoma cells were grown in McCoy's 5A medium with 10% FBS. HCT116 and *RAD18*$^{-/-}$ HCT116 cells were a gift form Drs. N. Shiomi and H. Shiomi (27). HeLa cells were obtained from the Health Science Research Resources Bank. U2OS cells were obtained from the American Type Culture Collection (HTB-96).

RNA interference

We used the following siRNAs: siBRCA1 #1: GGAACCUGUCUCCACAAAG-dTdT (28); siBRCA1 #2: UCACAGUGUCCUUUAUGUA-dTdT (29); si53BP1: GAAGGACGGAGUACUAAUA-dTdT; siUBC13: Dharmacon siGENOME SMARTpool; siRNF8 #D: Dharmacon siGENOME SMARTpool; siRNF8 #2: GGAGAUAGCCCAAGGAGAA-dTdT (22; this siRNA sequence was not included in siRNF8 #D); siRNF168 #5: GACACUUUCUCCACAGAUA-UU; siRNF168 #C: GGCGAAGAGCGAUGGAAGA-dTdT (12); and siRAP80: CCAGUUGGAGGUUUAUCAA-dTdT (22). Nontargeting control siRNA (siCTRL) was purchased from Sigma-Aldrich (Mission SIC-002). For the simultaneous depletion of RNF8, RNF168, BRCA1, and 53BP1, siRNF8 (#D or #2), siRNF168 (#5 or #C), siBRCA1 (#1 or #2), and si53BP1 were mixed to final concentrations of 18 nmol/L, 18 nmol/L, 36 nmol/L, and 4.5 nmol/L, respectively. The total siRNA amount was adjusted to be the same in each sample by adding siCTRL. All RNAi transfections were carried out using Lipofectamine RNAiMAX (Invitrogen).

Generation of a siRNA-resistant RNF8-expressing vector

To generate RNF8 constructs resistant to siRNF8#2, we introduced the following underlined silent mutations in RNF8: GGAGATAGCCCAGGGCGAG.

Immunofluorescence microscopy

HCT116 and 293T cells were grown on MAS-coated No. 1 glass coverslips (Matsunami). HeLa and U2OS cells were grown on No. 1 glass coverslips (Fisher Scientific). The cells were fixed by incubation in 3% paraformaldehyde and 2% sucrose in PBS for 15 minutes at room temperature. They were permeabilized by incubation in 0.5% Triton X-100 in PBS for 15 minutes at room temperature. For BRCA1 immunofluorescence assays, the cells were preextracted with 0.2% Triton X-100 in PBS for

Published OnlineFirst August 3, 2012; DOI:10.1158/0008-5472.CAN-12-1057

5 minutes on ice and fixed using 3% paraformaldehyde and 2% sucrose in PBS. After fixation, the cells were washed with PBS 3 times and blocked with 2% bovine serum albumin (BSA) in PBS for 1 hour. The cells were then stained with the indicated antibodies, which were diluted in 2% BSA in PBS. For RPA immunofluorescence assays, the cells were preextracted with 0.5% Triton X-100 in CSK buffer [20 mmol/L Hepes (pH7.4), 50 mmol/L NaCl, 3 mmol/L $MgCl_2$, 300 mmol/L sucrose] for 5 minutes on ice and fixed using 3% paraformaldehyde and 2% sucrose in PBS. After fixation, cells were washed with PBS 3 times and blocked with 3% skim milk in 0.05% Tween-20 in PBS for 1 hour. The cells were then stained with anti-RPA antibodies, which were diluted in 1% BSA in PBS. The cells were washed with PBS twice and stained with Alexa Fluor 488 goat anti-mouse immunoglobulin G (IgG; Invitrogen), Alexa Fluor 555 goat anti-rabbit IgG (Invitrogen), or CF555 goat anti-chicken IgY (Biotium). The cells were washed with 2% BSA in PBS and PBS alone 2 times each. DNA was counterstained with 4′, 6-diamidino-2-phenylindole (0.2 μg/mL) in PBS, and samples were mounted with Prolong Gold mounting reagent (Invitrogen). Confocal images were captured using an inverted microscope (TCS SP5, Leica) equipped with a 63x oil immersion lens. A minimum of 300 cells or 100 53BP1 focus-negative cells (RNF168-knockdown) were analyzed per experiment. Images were acquired in LAS AF (Leica) format. Images were adjusted and combined using Photoshop (Adobe).

Western blotting

Cells were lysed in SDS sample buffer. Whole-cell lysates were separated using SDS-PAGE (5–20% e-PAGEL, ATTO) and transferred to nitrocellulose membranes using the iBlot Gel Transfer System (Invitrogen). Nitrocellulose membranes were blocked with 5% Difco skim milk (BD Biosciences) in TBST, blotted with the indicated primary antibodies and blotted with horseradish peroxidase (HRP)-conjugated secondary antibodies. The Western Lightning ECL Pro Reagent Kit (Perkin-Elmer) was used to detect chemiluminescent HRP-conjugated antibodies. Chemiluminescent signals were detected using a LAS4000 (Fuji Film) or ChemiDoc XRS^+ (BioRad).

Antibodies

We used the following primary antibodies: RAD51 (70-001 lot 1, Bio Academia, 1:20,000 for immunofluorescence and 1:2,000 for Western blotting; a gift from Dr. Kurumizaka, 1:4,000 for immunofluorescence; 70-005, Bio Academia, 1:2,000 for immunofluorescence), 53BP1 (clone 19, BD Biosciences, 1:5,000 for immunofluorescence and 1:2,000 for Western blotting), γ-H2AX (clone JBW301, Upstate, 1:5,000 for immunofluorescence), conjugated ubiquitin (clone FK2, Nippon Bio-Test Laboratories, 1:20,000 for immunofluorescence), RNF8 (B-2, Santa Cruz, 1:100 for Western blotting), BRCA1 (D-9, Santa Cruz, 1:200 for Western blotting; C-20, Santa Cruz, 1:100 for immunofluorescence), α-tubulin (T6074, Sigma-Aldrich, 1:1,000 for Western blotting), phospho-RPA32 Ser4/8 (A300-245A, Bethyl Laboratories, 1:1,000 for Western blotting), RPA32 (RPA34-19, Calbiochem, 5 μg/mL for immunofluorescence and Western blotting), UBC13 (ab25885, abcam, 1:1000), RAP80 (EPR5315, Epitomics, 1:10,000 for Western blotting), and RNF168 [RNF168-C (9), a gift from Dr. Durocher].

DR-GFP assay

A HeLa clone carrying the DR-GFP homologous recombination reporter was used for the analysis of homologous recombination. For analyses with siRNA, cells were transfected with the indicated siRNA and cultured in 6-well dishes for 48 hours. The cells were then transfected with 2 μg of pCBASce, the I-SceI expression plasmid using FuGene HD (Roche). The cells were collected 48 hours post-pCBASce transfection via trypsinization, washed twice with PBS, resuspended in 0.1% FBS/PBS, and filtered. The proportion of GFP-positive cells was determined using flow cytometry with a FACSCalibur flow cytometer (BD Biosciences).

Pharmacologic inhibition

Cells were incubated with 10 μmol/L KU55933 (Calbiochem) and 10 μmol/L NU7026 (Sigma) or 10 μmol/L MG132 (Sigma) for 1 hour before irradiation.

DNA damage

Cells were exposed to X-rays using an MBR-1520RX-ray irradiator (Hitachi Medico) or were treated with neocarzinostatin (Sigma-Aldrich).

Results

UBC13 is required for RAD51 assembly at DSB sites, but RNF8 and RNF168 are not

UBC13 is an essential E2 ubiquitin-conjugating enzyme for RAD51 assembly at DSBs (5). Upon DSBs formations, UBC13 cooperates with E3 ubiquitin ligases (RNF8 and RNF168) to generate Lys 63-linked ubiquitin chains on damaged chromatin (2, 6–11). Therefore, we predicted that not only UBC13 but also RNF8 and RNF168 would be required for RAD51-dependent homologous recombination. To test this hypothesis, UBC13, RNF8, or RNF168 was depleted from U2OS cells by using siRNA transfection (Supplementary Fig. S2) and RAD51 accumulation at DSB sites was analyzed by immunofluorescence. Cells transfected with UBC13-, RNF8-, or RNF168-specific siRNAs showed a complete deficiency of 53BP1 focus formation at DSB sites, indicating effective knockdown of these genes (Fig. 1A). RAD51 focus formation was also defective in UBC13-depeleted cells (Fig. 1A and B). Nevertheless, RAD51 was recruited to DSB sites in RNF8- or RNF168-depleted cells (Fig. 1A and B). To further confirm the RNF8-independent recruitment of RAD51 to DSB sites, $RNF8^{-/-}$ MEFs and matched WT MEFs were treated with neocarzinostatin, a compound that specifically induces DSBs, and stained with anti-RAD51 antibody. RAD51 foci were observed in $RNF8^{-/-}$ MEFs, but these foci were smaller than those observed in WT MEFs (Supplementary Fig. S3). Thus, UBC13 is essential for RAD51 assembly at DSB sites, but RNF8 and RNF168 are not.

BRCA1 regulates RAD51 assembly in RNF8-depleted cells

BRCA1 forms several independent protein complexes. The BRCA1-A complex binds through the 2 UIMs of RAP80 to the

Published OnlineFirst August 3, 2012; DOI:10.1158/0008-5472.CAN-12-1057

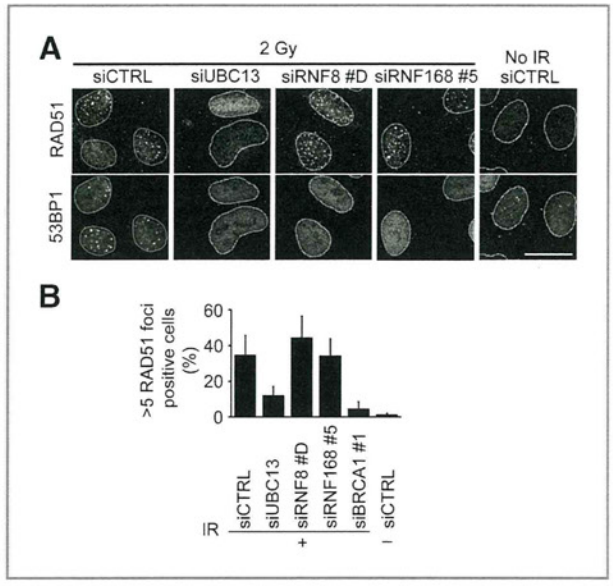

Figure 1. UBC13, but not RNF8 or RNF168, is required for RAD51 assembly at DSB sites. A and B, U2OS cells transfected with the indicated siRNAs were irradiated with 2 Gy and the immunofluorescence of RAD51 and 53BP1 was analyzed at 6 hours postirradiation. A, representative images. Nuclei are indicated by lines. Scale bar, 25 μm. B, the quantification of cells with more than 5 RAD51 foci (mean ± SD; $N = 3$). IR, irradiation.

RNF8/RNF168-generated Lys 63-linked ubiquitin chain (2, 6–8, 11, 17–20). Therefore, the irradiation-induced foci (IRIF) of BRCA1 are significantly diminished in RNF8- and RNF168-depleted cells. However, other BRCA1 complexes are recruited to DSB sites in a RAP80-independent manner (21, 22), and these complexes promote RAD51 assembly at DSB sites. These results imply that a small subset of BRCA1 protein might be recruited to DSB sites in the absence of RNF8 (Supplementary Fig. S1D and S1E). To test this possibility, we conducted a preextraction before cell fixation to detect a small amount of chromatin-bound BRCA1 accumulation. RNF8- or RAP80-depleted cells contained BRCA1 foci, but these foci were smaller than the foci observed in control cells (Fig. 2A and Supplementary Fig. S2B). This result was consistent with the observation that BRCA1, but not 53BP1 or conjugated ubiquitin, weakly accumulates at microlaser-generated DSB tracks in RNF8-depleted cells (7) and RNF168-depleted cells (10). These data led us to hypothesize that the small amount of BRCA1 at DSB sites might promote RAD51 assembly in RNF8-depleted cells (Supplementary Fig. S1E). As a result, we analyzed the impact of BRCA1 depletion on RNF8-depleted cells. The effective and simultaneous knockdown of RNF8 and BRCA1 was confirmed using Western blotting (Fig. 2B). The depletion of BRCA1 significantly inhibited RAD51 assembly in HCT116 cells, indicating that BRCA1 knockdown was sufficient to inhibit BRCA1-dependent RAD51 assembly (Supplementary Fig. S1B). The depletion of BRCA1 significantly suppressed irradiation-induced RAD51 assembly in RNF8-depleted cells (Fig. 2C and D). As cell-cycle distribution was comparable among cells transfected with various combinations of nontargeting, BRCA1- and RNF8-specific siRNAs, it is unlikely that the percentage of RAD51 focus-positive cells was affected by the ratio of cells in S-G_2 phase (Supplementary Fig. S4A). These results indicate that BRCA1 promotes RAD51 assembly independently of RNF8-dependent chromatin ubiquitination.

RAD51 is recruited to DSB sites in BRCA1/53BP1-depleted human cells

Loss of 53BP1 IRIF restores RAD51 assembly in cells derived from BRCA1 hypomorphic ($BRCA1^{\Delta 11/\Delta 11}$) mice (24, 25; see also Supplementary Fig. S1C). In contrast, depletion of RNF8 from BRCA1-depleted human HCT116 cells resulted in loss of 53BP1 IRIF, but this depletion did not restore RAD51 foci (Fig. 2C and Supplementary Fig. S1F). These data appear to be contradictory. This discrepancy may result from differences between murine and human cells. Therefore, we next examined whether the simultaneous silencing of 53BP1 and BRCA1 gene expression using siRNAs could rescue the loss of RAD51 foci in BRCA1-depleted human cells. To avoid off-target siRNA effects, 2 different BRCA1-specific siRNAs were used for the experiments. The silencing of 53BP1 in the BRCA1-depleted cells restored RAD51 assembly at DSB sites (Supplementary Fig. S5A and S5B). The efficiency of BRCA1 knockdown in cells concomitantly transfected with 53BP1- and BRCA1-specific siRNAs was equivalent to the knockdown efficiency in cells transfected with both the nontargeting siRNA and the identical BRCA1-specific siRNA (Supplementary Fig. S5C). Furthermore, the restored RAD51 focus formation was not due to a change in the cell-cycle distribution (Supplementary Fig. S4B). These data indicate that BRCA1 is dispensable for RAD51 assembly at DSB sites in 53BP1-depleted human cells, reproducing previous results found using $BRCA1^{\Delta 11/\Delta 11}$ murine cells (24, 25).

RNF8-dependent chromatin ubiquitination is required for RAD51 assembly in BRCA1/53BP1-depleted cells

No BRCA1 or 53BP1 focus formation was observed in either BRCA1/53BP1-depleted cells or RNF8/BRCA1-depleted cells. However, these cells showed a sharp contrast in the efficiency of RAD51 assembly at DSB sites: 53BP1/BRCA1-depleted cells displayed efficient RAD51 IRIF whereas RNF8/BRCA1-depleted cells did not (Supplementary Fig. S1C and S1F). These results suggest that RAD51 assembly in BRCA1/53BP1-depleted cells may depend on RNF8. To test this hypothesis, RNF8 was concomitantly depleted with BRCA1 and 53BP1 in HCT116 cells, and the impact of RNF8 depletion on RAD51 assembly at DSB sites in BRCA1/53BP1-depleted cells was monitored. The effective and simultaneous depletion of RNF8, BRCA1, and 53BP1 was confirmed using Western blotting (Fig. 3A), and the effective knockdown of RNF8 was also confirmed in terms of DNA damage response signaling by the observation of defective conjugated-ubiquitin IRIF, as visualized using the FK2 antibody (Fig. 3B). The depletion of RNF8 from BRCA1/53BP1-depleted cells did not reduce the amount of S-G_2 phase cells (Supplementary Fig. S4C) or affect the amount RAD51 protein (Fig. 3A), but it strongly suppressed RAD51 assembly at DSB sites (Fig. 3B and C). Two different RNF8-specific siRNAs showed a similar inhibitory effect on RAD51 IRIF in BRCA1/53BP1-depleted cells, excluding the possibility of off-target

Published OnlineFirst August 3, 2012; DOI:10.1158/0008-5472.CAN-12-1057

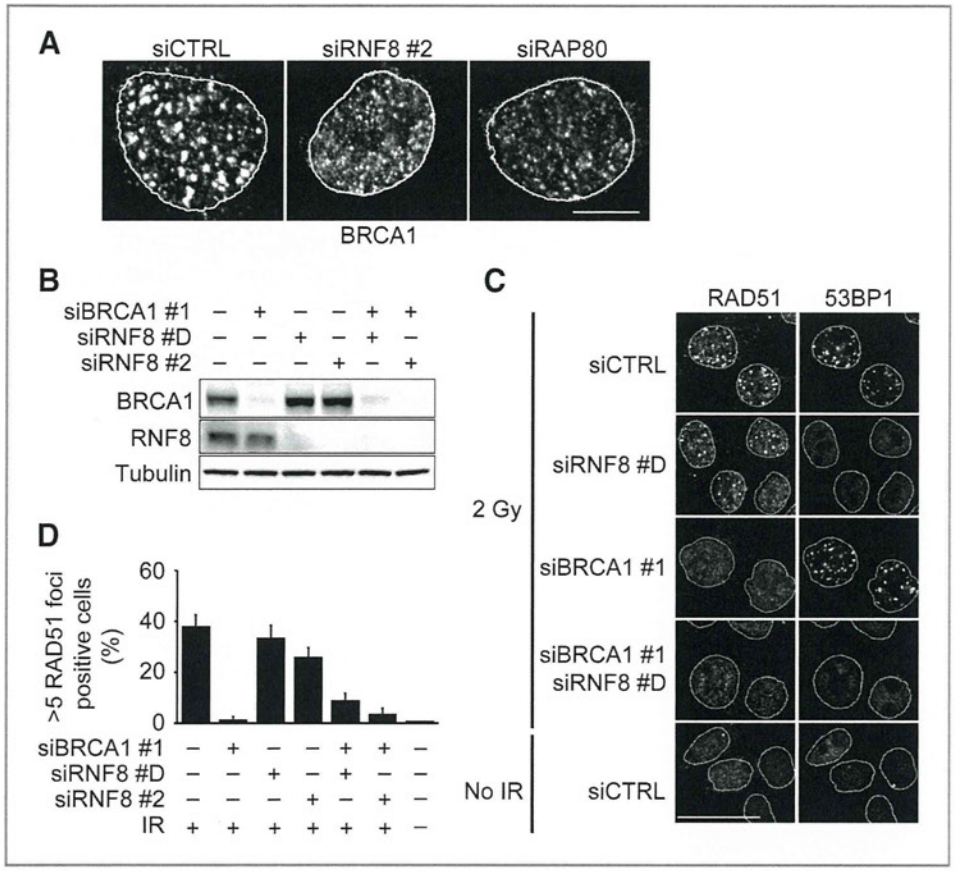

Figure 2. RNF8-independent RAD51 assembly is regulated by BRCA1. A, HeLa cells transfected with the indicated siRNAs were irradiated with 2 Gy, and the immunofluorescence of BRCA1 was analyzed at 4 hours postirradiation. Representative images. Nuclei are indicated by lines. Scale bar, 10 μm. B–D, HCT116 cells transfected with the indicated siRNAs were subjected to Western blotting for the indicated proteins (B) or irradiated with 2 Gy, and the immunofluorescence of RAD51 and 53BP1 was analyzed at 6 hours postirradiation. Representative images. Nuclei are indicated by lines. C, scale bar, 25 μm. D, the quantification of cells with more than 5 RAD51 foci (mean ± SD; $N = 3$). IR, irradiation.

effects of the RNF8-specific siRNAs. The depletion of RNF8 also suppressed RAD51 IRIF in BRCA1/53BP1-depleted HeLa and 293T cells (Supplementary Fig. S6).

RNF8 is recruited to DSB sites through binding to phospho-MDC1 with its forkhead-associated (FHA) domain; the protein then ubiquitinates the chromatin surrounding the DSBs through a mechanism that depends on its RING finger domain (6–8). To explore the roles of RNF8 in RAD51 assembly at DSB sites in the absence of BRCA1 and 53BP1, we simultaneously knocked down RNF8, BRCA1, and 53BP1 and transiently reintroduced the following siRNA-resistant forms of RNF8 into 293T cells: WT GFP-RNF8, FHA mutant ($RNF8^{R42A}$), and RING mutant ($RNF8^{C403S}$). The cells were irradiated and processed for RAD51 immunofluorescence. In this assay, we only analyzed cells with weak GFP-RNF8 expression because overexpression of GFP-RNF8 suppressed RAD51 assembly even in control cells. Neither the reintroduction of $RNF8^{C403S}$ nor $RNF8^{R42A}$ restored RAD51 assembly efficiency to the levels observed with WT RNF8 (Fig. 3D and E). These data strongly suggest that RNF8-dependent ubiquitination is required for BRCA1-independent RAD51 assembly in 53BP1-depleted cells.

The recruitment of RNF8 to DSB sites is dependent on ATM (6–8). This led us to examine whether the inhibition of ATM suppressed RAD51 assembly at DSB sites in BRCA1/53BP1-depleted cells. The activities of ATM and DNA-PK are redundant (30); therefore, we treated cells with a combination of an ATM-specific kinase inhibitor KU55933 and a DNA-PK-specific inhibitor NU7026. The pharmacologic inhibition of the kinase activities of ATM and DNA-PK suppressed RAD51 focus formation in BRCA1/53BP1-depleted cells. The suppressive effect on RAD51 assembly observed in control cells was less efficient than the suppressive effect observed in BRCA1/53BP1-depleted cells (Fig. 4A and B). These data most likely indicate that the suppressive effect of RNF8 depletion on RAD51 IRIF formation is restricted to BRCA1-depleted cells (Figs. 1–3). In contrast, MG132, a protein that inhibits ubiquitin recycling and ubiquitination-dependent DSB signaling (31), completely inhibited RAD51 focus formation in both BRCA1/53BP1-depleted and control cells (Fig. 4A and B). This inhibition most likely occurred because the UBC13-dependent ubiquitination pathway is indispensable for RAD51 assembly (Fig. 1; refs. 5, 32).

We next monitored homologous recombination to obtain more direct evidence for the role of RNF8 in BRCA1-independent homologous recombination. To measure frequency of homologous recombination, we used DR-GPF assay (26). In this assay, a direct repeat of a full-length GFP mutated to contain a restriction enzyme (I-SceI) recognition site and a 5′- and 3′-truncated GFP were integrated into the genome of HeLa cells. A DSB was generated at the I-SceI site by transfection of I-SceI expression vectors. Cells that repaired the DSB by homologous recombination using 5′- and 3′-truncated GFP as a template expressed WT GFP and exhibited green fluorescence beyond levels of autofluorescence. Compared with control siRNA transfected cells, the depletion of BRCA1 led to a

Published OnlineFirst August 3, 2012; DOI:10.1158/0008-5472.CAN-12-1057

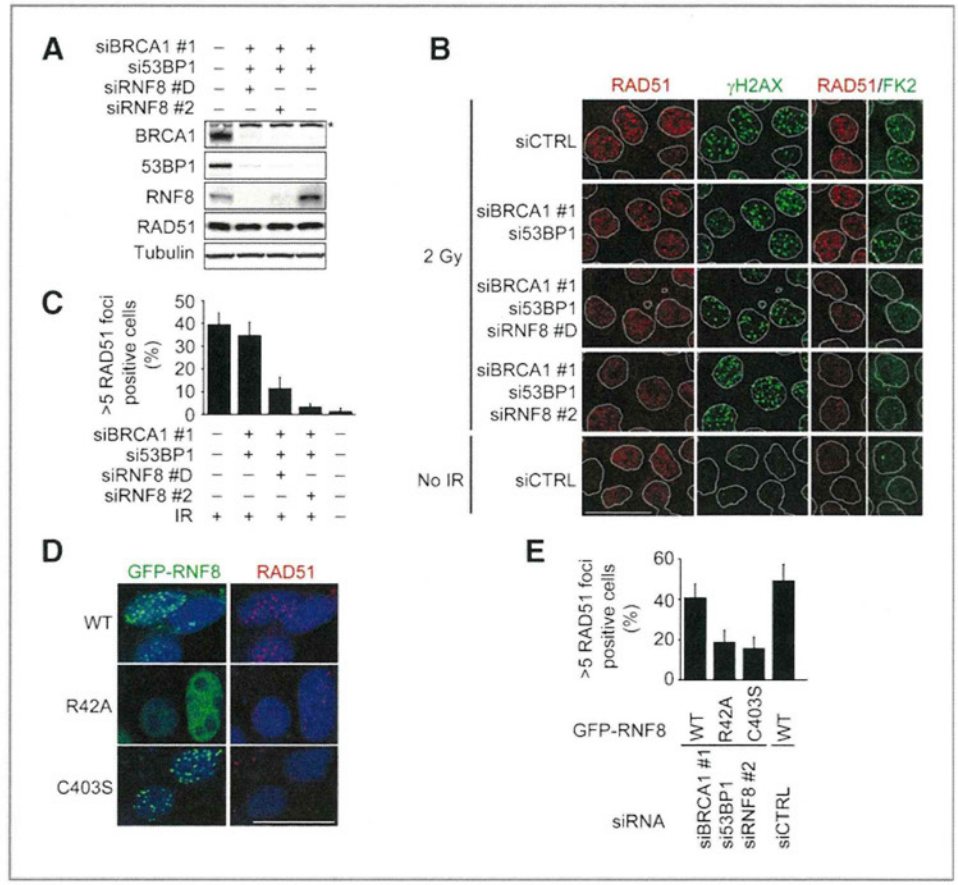

Figure 3. RNF8 regulates RAD51 assembly in BRCA1/53BP1-depleted cells. A–C, HCT116 cells transfected with the indicated siRNAs were subjected to Western blotting for the indicated proteins (A) or irradiated with 2 Gy and analyzed for RAD51 and conjugated ubiquitin (FK2) or γH2AX immunofluorescence at 6 hours postirradiation. Representative images. Nuclei are indicated by lines. B, scale bar, 25 μm. C, the quantification of cells with more than 5 RAD51 foci (mean ± SD; $N = 3$). D and E, siRNA-resistant GFP-RNF8 WT, R42A, or C403S was reintroduced into 293 T cells transfected with siRNF8#2, siBRCA1#1, and si53BP1 or siCTRL. The cells were irradiated with 2 Gy and analyzed for RAD51 immunofluorescence at 4 hours postirradiation. Representative images. D, scale bar, 25 μm. E, the quantification of cells with more than 5 RAD51 foci and weak GFP-RNF8 expression (mean ± SD; $N = 3$). *, nonspecific bands. IR, irradiation.

significant reduction in the frequency of GFP-positive cells and the concomitant depletion of 53BP1 and BRCA1 did not reduce the frequency of GFP-positive cells. However, when RNF8, BRCA1, and 53BP1were concomitantly depleted, the frequency of GFP positive cells was decreased as comparable to BRCA1-depleted cells (Fig. 4C and D). Thus, RNF8 regulates homologous recombination in BRCA1/53BP1-depleted cells.

RNF168 is required for RAD51 assembly in BRCA1/53BP1-depleted cells

The E3 ligase activity of RNF8 is a prerequisite for RNF168/UBC13-mediated Lys 63-linked ubiquitin chain formation on histone H2A (9, 10) and RNF168-dependent turnover of histone demethylase JMJD2A, JMJD2B (14), and a polycomb protein L3MBTL1 (13) at DSB sites. On the other hand, RNF8 but not RNF168 is required for Lys 48-linked ubiquitin chain formation, which promotes KU80 degradation (15). Therefore, we examined whether RNF168 was required for RAD51 IRIF formation in BRCA1/53BP1-depleted cells. The protein levels of RNF168 were significantly suppressed when cells were concomitantly transfected with RNF168-, BRCA1-, and 53BP1-specific siRNAs (Supplementary Fig. S2). However, this RNF168 reduction was not sufficient to completely inhibit the 53BP1 IRIF that is mediated by RNF168. Thus, we analyzed RAD51 IRIF in cells without 53BP1 foci. Two different RNF168-specific siRNAs (#5 and #C) were used for this experiment, and both siRNAs clearly suppressed RAD51 IRIF in BRCA1/53BP1-depleted cells (Fig. 5A and B). These data indicate that both RNF8 and RNF168 promote RAD51 assembly in BRCA1/53BP1-depleted cells.

RNF8 is not required for DNA end resection in BRCA1/53BP1-depleted cells

RAD18 is an important E3 ubiquitin ligase for postreplication repair at stalled replication forks (11). In addition, RAD18 binds to RNF8-dependent ubiquitin chains at irradiation-induced DSBs, recruits RAD51C to DSB sites and promotes homologous recombination when cells are exposed to irradiation. The recruitment of RAD18 to DSB sites is independent of BRCA1 (33). Therefore, we tested whether RAD18 is required for RNF8-dependent RAD51 assembly in BRCA1/53BP1-depleted cells. *RAD18*$^{-/-}$ HCT116 cells (27) showed clear irradiation-induced RAD51 foci after the depletion of BRCA1 and 53BP1: this focus formation was comparable to *RAD18*$^{+/+}$ HCT116 cells (Supplementary Figs. S5 and S7), suggesting that RAD18 is dispensable for the BRCA1-independent assembly of RAD51.

During homologous recombination, DSB edges are resected to form a 3′ overhang. RPA is loaded onto the ssDNA, phosphorylated and displaced from single-stranded DNA by RAD51 (3). BRCA1 promotes induction of the ssDNA overhang (34), and 53BP1 inhibits the resection (25). Therefore, BRCA1-depleted cells show defective homologous recombination, and

Published OnlineFirst August 3, 2012; DOI:10.1158/0008-5472.CAN-12-1057

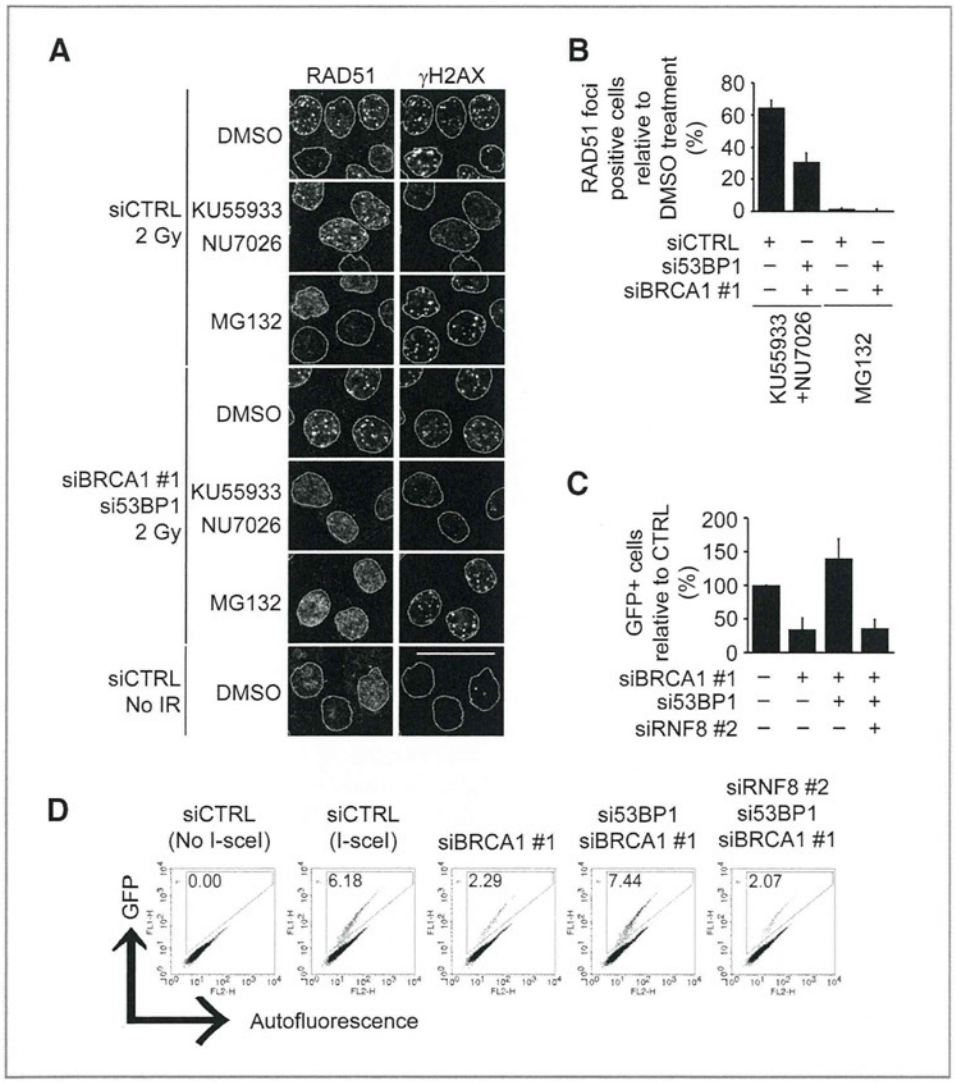

Figure 4. RNF8 regulates homologous recombination in BRCA1/53BP1-depleted cells. A and B, HCT116 cells transfected with the indicated siRNAs were treated with KU55933+NU7026, MG132, or dimethyl sulfoxide for 1 hour and then irradiated with 2 Gy and analyzed for RAD51 and γH2AX immunofluorescence at 4 hours postirradiation. Nuclei are indicated by lines. A, scale bar, 25 μm. B, the quantification of cells with more than 5 RAD51 foci (mean ± SD; $N = 3$). C and D, cells transfected with the indicated siRNAs were subjected to the DR-GFP assay. The quantification of cells with GFP expression (mean ± SD; $N = 3$). D, representative data from flow cytometry. DMSO, dimethyl sulfoxide; IR, irradiation

knockdown of 53BP1 restores homologous recombination in BRCA1-depleted cells. Intriguingly, RPA formed foci in neocarzinostatin-treated RNF8/BRCA1/53BP1-depleted cells (Fig. 6A). Furthermore, substantial levels of phosphorylated RPA were detected not only in control or BRCA1/53BP1-depleted cells but also in RNF8/BRCA1/53BP1-depleted cells after irradiation (Fig. 6B). These data indicate that RNF8 is required for RAD51 assembly but not for DNA end resection and RPA assembly at DSB sites in BRCA1/53BP1-depleted cells.

Discussion

DNA damage-dependent chromatin ubiquitination has an important role as a signal transducer in the DNA DSB response. The depletion of RNF8 or RNF168 suppresses the accumulation of 53BP1 and BRCA1 at DSB sites and induces an aberrant G_2–M checkpoint and hyper-radiosensitivity (6–10). Furthermore, biallelic mutations in RNF168 have been found in radiosensitive primary immunodeficiency (RIDDLE syndrome or RNF168 deficiency) patients (9, 35, 36), and RNF8-knockout mice display decreased levels of serum IgG, chromosomal aberration, radiosensitivity, impaired spermatogenesis, and increased cancer predisposition (37–39). Owing to their physiologic importance, the roles of RNF8 and RNF168 in DNA repair are being extensively studied. One important role of RNF8-/RNF168-dependent chromatin ubiquitination in DNA repair is the fine-tuning of DNA end resection. The K63-linked ubiquitin chain generated by RNF8 and RNF168 promotes the recruitment of the BRCA1-A complex through the tandem UIM of RAP80 by specific binding to the Lys 63-linked ubiquitin chain (6–10, 17–20); this chain retains excess BRCA1 at a position slightly distant from the edges of DSBs and suppresses excessive DSB end processing (21, 22). In contrast, BRCA1 also forms complexes with the homologous recombination factors and accumulates at DSB sites in a RAP80-independent manner (2). In addition to the generation of Lys 63-linked ubiquitin chains at DSB sites, RNF8 plays other roles in DNA repair. RNF8 and RNF168 promote ubiquitination-dependent turnover of JMJD2A, JMJD2B (14), and L3MBTL1 (13) at DSB sites. The loss of chromatin-bound JMJD2A, JMJD2B, and L3MBTL1 exposes

Published OnlineFirst August 3, 2012; DOI:10.1158/0008-5472.CAN-12-1057

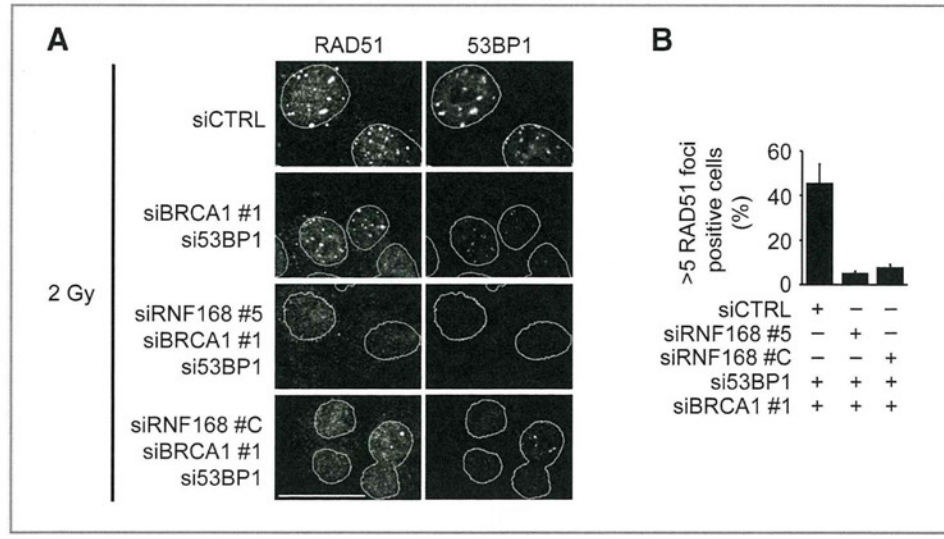

Figure 5. RNF168 regulates RAD51 assembly in BRCA1/53BP1-depleted cells. A and B, HCT116 cells transfected with the indicated siRNAs were irradiated with 2 Gy and analyzed for RAD51 and 53BP1 immunofluorescence at 6 hours postirradiation. Representative images. Nuclei are indicated by lines. A, scale bar, 25 μm. The quantification of cells with more than 5 RAD51 foci (mean ± SD; $N = 3$). B, cells with small 53BP1 foci (transfected with siCTRL, si53BP1, and siBRCA1) or cells without 53BP1 foci (transfected with siRNF168, si53BP1 and siBRCA1) were analyzed.

Lys-20 di-methylated histone H4 and promotes the binding of 53BP1 to the Lys-20 di-methylated histone H4 at DSB sites. RNF8 also promotes the degradation of KU80 at DSB sites (15) and RNF4-dependent/proteasome-mediated turnover of MDC1 and RPA at DSB sites (40). The degradation of KU80 at DSB sites facilitates NHEJ (15). The depletion of RNF4 results in decreased efficiency of homologous recombination and NHEJ. Furthermore, RNF8 recruits a chromatin remodeling factor, chromodomain helicase DNA-binding protein 4 (CHD4), independently of its E3 ubiquitin ligase activity and the canonical phosphoprotein-binding property of the FHA domain and thereby promotes chromatin decondensation (16).

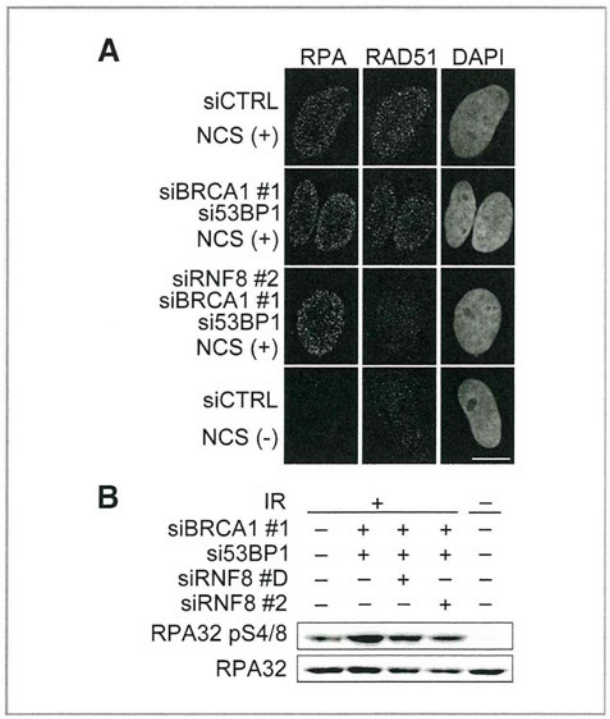

Figure 6. RNF8 promotes the displacement of RPA by RAD51 after DNA end resection in BRCA1/53BP1-depleted cells. A, HeLa cells transfected with the indicated siRNA were treated with 100 ng/mL NCS for 15 minutes and then subjected to immunofluorescence with the indicated antibodies at 5 hours post-neocarzinostatin treatment. Scale bar, 10 μm. B, HCT116 cells transfected with the indicated siRNAs were irradiated with 20 Gy and subjected to Western blotting for the indicated proteins at 4 hours postirradiation.

In this study, we showed that RNF8 promotes RAD51 assembly at DSB sites in BRCA1/53BP1-depleted cells (Fig 3), although Lys 63-linked ubiquitination is dispensable for RAD51 assembly in the presence of BRCA1. The accumulation of RPA at neocarzinostatin-induced DSBs and the irradiation-induced phosphorylation of RPA (Fig. 6) suggest that RNF8 is not required for nuclease accessibility to DSBs in BRCA1/53BP1-depleted cells. These data indicate that RNF8 functions downstream of RPA and upstream of RAD51-ssDNA filament formation during homologous recombination signaling. RNF8 is likely to promote the displacement of RPA by RAD51. We propose 2 models that explain the phenomenon: (i) RNF8/RNF168-dependnet histone H2A ubiquitination induces local structural changes in chromatin and create a space allowing RPA displacement by RAD51 in BRCA1/53BP1-depleted cells. (ii) Some substrates, which restrict the displacement of RPA by RAD51, may be ubiquitinated by RNF8 and/or RNF168, and removed from DSB sites by VCP/p97, proteasome or others, as recent studies revealed that RNF8- and/or RNF168-dependent ubiquitination induces protein turnover at DSB sites (12–15, 40). Even in the case where RNF8 have such functions, their functions are not obvious in the presence of BRCA1. BRCA1 probably has ability to promote RAD51 assembly without the support of RNF8 and RNF168. The requirement of RNF8 E3 ubiquitin ligase activity for RAD51 assembly in BRCA1/53BP1-depleted cells suggests that RNF8/CHD4-dependent chromatin unfolding (16) is not sufficient for the displacement of RPA by RAD51.

BRCA1-independent DNA end resection is restricted by 53BP1, but end resection functions properly when the restriction imposed by 53BP1 is lifted. Therefore, in the absence of 53BP1, BRCA1 is not required for DNA end resection and

Published OnlineFirst August 3, 2012; DOI:10.1158/0008-5472.CAN-12-1057

RAD51 assembly (25). This suggests that BRCA1 actively promotes the recruitment of resection factors, such as CtIP and MRE11, to overcome the jamming effect of 53BP1. In RNF8- or RNF168-depleted cells, 53BP1 is not recruited to DSB sites. Therefore, DNA end resection is not inhibited by 53BP1. Nevertheless, RAD51 assembly requires BRCA1 in RNF8-depleted cells. Furthermore, RNF8-/BRCA1-/53BP1-depleted cells do not show RAD51 assembly at DSB sites. These findings suggest that BRCA1 also actively promotes RPA displacement by RAD51 in RNF8-depleted cells.

RAD51 assembles at DSB sites in the absence of chromatin ubiquitination by RNF8 and RNF168 at DSB sites (Figs. 1 and 2). Nevertheless, ubiquitination is an essential posttranslational modification for RAD51 assembly at DSB sites because the depletion of UBC13 and the inhibition of ubiquitin recycling using MG132 completely suppress RAD51 IRIF (Fig. 4; ref. 32). These findings suggest that another E3 ligase may weakly (because ubiquitin conjugation is not detected in RNF8- or RNF168-depleted cells) ubiquitinate some substrates, whose ubiquitination is required for RAD51 assembly at the damaged chromatin in the absence of either RNF8 or RNF168. One of the candidate E3s is BRCA1. BRCA1 forms a ubiquitin chain at sites of DNA damage (41) and ubiquitinates histone H2A to maintain heterochromatin structure (42). Nevertheless, the E3 ligase activity of BRCA1 is not required for RAD51 assembly at DSB sites in ES cell (43). In addition, the E3 ubiquitin ligase activity of BRCA1 is not required for tumor suppression, but the BRCA1-BARD1 interaction through the RING domain is important for this activity (44, 45). These lines of evidence do not support the conclusion that BRCA1-dependent ubiquitination promotes homologous recombination in the presence of RNF8. However, we can speculate a model in which BRCA1 and RNF8 are redundant for the ubiquitination of some proteins and that BRCA1-dependent ubiquitination gains in importance in homologous recombination only when RNF8 is depleted.

Our data predict that the pharmacologic inhibition of RNF8 or RNF168 would suppress homologous recombination only in BRCA1-mutated/53BP1^{low} cancer cells but not in healthy cells. In addition, ATM/DNA-PK inhibition would suppress homologous recombination more effectively in BRCA1-mutated/53BP1^{low} cancer cells than in healthy cells. If these predictions are correct, the combination of DNA-damaging agents and the inhibition of RNF8, RNF168, or ATM may be useful as a cancer therapy. However, RNF8 is required for resistance not only to irradiation (6–8) but also to hydroxyurea and aphidicolin treatment (46). Therefore, a careful examination should be conducted to determine which DNA-damaging agents can be combined with RNF8 inhibition for cancer chemotherapy.

Disclosure of Potential Conflicts of Interest

No potential conflicts of interest were disclosed.

Authors' Contributions

Conception and design: S. Nakada
Development of methodology: S. Nakada
Acquisition of data (provided animals, acquired and managed patients, provided facilities, etc.): S. Nakada
Analysis and interpretation of data (e.g., statistical analysis, biostatistics, computational analysis): S. Nakada
Writing, review, and/or revision of the manuscript: S. Nakada, K. Matsuo
Administrative, technical, or material support (i.e., reporting or organizing data, constructing databases): S. Nakada, R.M. Yonamine

Acknowledgments

The authors are grateful to H. Kurumizaka (Waseda University) for kindly providing the RAD51 antibody; N. Shiomi and H. Shiomi for kindly providing the RAD18-knockout HCT116 cells; D. Durocher for kindly providing the RNF168 antibody and the RNF8 knockout and matched WT MEFs; J. Lukas for kindly providing the RNF8 cDNA; M. Jasin, A. Ui, H. Ogiwara, J. Kobayashi, and K. Komatsu for the DR-GFP HeLa cells; A. Kato for technical advice; and R. Sakasai for critical reading of the manuscript.

Grant Support

This work was supported by the Promotion of Environmental Improvement for Independence of Young Researchers 'Kanrinmaru Project' and KAKENHI from the Ministry of Education, Culture, Sports, Science and Technology (MEXT), Japan, as well as the Kanae Foundation for the Promotion of Medical Research and the Sagawa Foundation for Promotion of Cancer Research.

The costs of publication of this article were defrayed in part by the payment of page charges. This article must therefore be hereby marked *advertisement* in accordance with 18 U.S.C. Section 1734 solely to indicate this fact.

Received March 22, 2012; revised July 13, 2012; accepted July 17, 2012; published OnlineFirst August 3, 2012.

References

1. Sonoda E, Hochegger H, Saberi A, Taniguchi Y, Takeda S. Differential usage of non-homologous end-joining and homologous recombination in double strand break repair. DNA Repair 2006;5:1021–9.
2. Ohta T, Sato K, Wu W. The BRCA1 ubiquitin ligase and homologous recombination repair. FEBS Lett 2011;585:2836–44.
3. Zou Y, Liu Y, Wu X, Shell SM. Functions of human replication protein A (RPA): from DNA replication to DNA damage and stress responses. J Cell Physiol 2006;208:267–73.
4. Helleday T. The underlying mechanism for the PARP and BRCA synthetic lethality: clearing up the misunderstandings. Mol Oncol 2011;5:387–93.
5. Zhao GY, Sonoda E, Barber LJ, Oka H, Murakawa Y, Yamada K, et al. A critical role for the ubiquitin-conjugating enzyme Ubc13 in initiating homologous recombination. Mol Cell 2007;25:663–75.
6. Huen MS, Grant R, Manke I, Minn K, Yu X, Yaffe MB, et al. RNF8 transduces the DNA-damage signal via histone ubiquitylation and checkpoint protein assembly. Cell 2007;131:901–14.
7. Mailand N, Bekker-Jensen S, Faustrup H, Melander F, Bartek J, Lukas C, et al. RNF8 ubiquitylates histones at DNA double-strand breaks and promotes assembly of repair proteins. Cell 2007;131:887–900.
8. Kolas NK, Chapman JR, Nakada S, Ylanko J, Chahwan R, Sweeney FD, et al. Orchestration of the DNA-damage response by the RNF8 ubiquitin ligase. Science 2007;318:1637–40.
9. Stewart GS, Panier S, Townsend K, Al-Hakim AK, Kolas NK, Miller ES, et al. The RIDDLE syndrome protein mediates a ubiquitin-dependent signaling cascade at sites of DNA damage. Cell 2009;136:420–34.
10. Doil C, Mailand N, Bekker-Jensen S, Menard P, Larsen DH, Pepperkok R, et al. RNF168 binds and amplifies ubiquitin conjugates on damaged chromosomes to allow accumulation of repair proteins. Cell 2009;136:435–46.
11. Al-Hakim A, Escribano-Diaz C, Landry MC, O'Donnell L, Panier S, Szilard RK, et al. The ubiquitous role of ubiquitin in the DNA damage response. DNA Repair 2010;9:1229–40.